Fatma Kübra CANITEZ

M.S. Thesis In Chemistry

July 2010

SYNTHESIS OF PORPHYRIN COATED NANOPARTICLES

by

Fatma Kübra CANITEZ

July 2010

SYNTHESIS OF PORPHYRIN COATED GOLD NANOPARTICLES

by

Fatma Kübra Canıtez

A thesis submitted to

the Graduate Institute of Science and Engineering

of

Fatih University

in partial fulfillment of the requirements for the degree of

Master of Science

in

Chemistry

July 2010
Istanbul, Turkey

APPROVAL PAGE

I certify that this thesis satisfies all the requirements as a thesis for the degree of Master of Science.

_____
Prof. Dr. Ayhan Bozkurt
Head of Department

This is to certify that I have read this thesis and that in my opinion it is fully adequate, in scope and quality, as a thesis for the degree of Master of Science.

_____
Assist. Prof. Ramazan ÖZTÜRK
Supervisor

Examining Committee Members

Assist. Prof. Ramazan ÖZTÜRK _____

Assist. Prof. Ergün GONCA _____

Assoc. Prof. Bayram ÜNAL _____

It is approved that this thesis has been written in compliance with the formatting rules laid down by the Graduate Institute of Sciences and Engineering.

_____
Assoc. Prof. Nurullah ARSLAN
Director

SYNTHESIS OF PORPHYRIN COATED GOLD NANOPARTICLES

Fatma Kübra Canıtez

M. S. Thesis - Chemistry
July 2010

Supervisor: Assist. Prof. Ramazan ÖZTÜRK

ABSTRACT

Porphyrin coated nanoparticles, especially gold nanoparticles (AuNPs), have much attention because of their potential use in Photodynamic Therapy (PDT). In this study, our aim was the coating of thiol-tailored meso-tetra(p-hydroxyphenyl)porphyrin and meso-tetra(m-hydroxyphenyl)porphyrin on to gold nanoparticles. Potassium thio acetate was used as a linker between the porphyrin ligands and AuNPs due to easily dissociating to form S-Au bonds. The synthesis of thiol-tailored porphyrin- AuNPs compounds were synthesized by one-pot reduction of $HAuCl_4$ by using $NaBH_4$ as a reducing agent. To compare the size of the tetradentate ligands-AuNPs, 4-tert-butyl phenol was used as a monodentate passivant. Thiol-tailored porphyrins were characterized by FTIR, MASS and NMR, and the porphyrin-AuNPs compounds were characterized by TEM, XRD and XPS.

Keywords: Porphyrins, Gold Nanoparticles**.**

PORFİRİN KAPLI ALTIN NANOPARÇACIKLARIN SENTEZİ

Fatma Kübra Canıtez

Yüksek Lisans Tezi - Kimya
Temmuz 2010

Tez yöneticisi: Yrd. Doç. Dr. Ramazan ÖZTÜRK

ÖZ

Porfirin kaplı nanoparçacıklar, özellikle altın nanoparçacıklar (AuNPs), Fotodinamik Terapi'de (PDT) kullanılmaları bakımından oldukça ilgi çekerler. Bu çalışmada, tiyol grupları bağlı meso-tetra(p-hidroksifenil)porfirin ve meso-tetra(m-hidroksifenil)porfirinlerinin sentezlenmesi ve altın nanoparçacıklar üzerine kaplanması hedeflenmiştir. Potasyum tiyo asetat, altın nanoparçacıkları ile kolaylıkla S-Au bağı oluşturabildikleri için, porfirin molekülleriyle altın nanoparçacıkları arasında bağlayıcı olarak kullanılmıştır. Porfirin-AuNPs yapıları, indirgen madde olarak $NaBH_4$ kullanılarak $HAuCl_4$ maddesinin indirgenmesiyle gerçekleşmiştir. Tek dişli ligand-AuNPs yapısından daha küçük boyutta olan dört dişli ligand-AuNPs yapılarının boyutlarını kontrol etmek için, 4-ter-bütil fenol, tek dişli ligand olarak kullanılmıştır. Tiyol bağlı porfirinler, FTIR, MASS ve NMR cihazları ile analiz edilirken, porfirin-AuNPs yapılarını analiz etmek için TEM, XRD ve XPS kullanılmıştır.

Anahtar Kelimeler: Porfirinler, Altın Nanoparçacıklar

ACKNOWLEDGMENT

First of all I would like to thank my supervising tutor, Assist. Prof. Ramazan Öztürk for his abundant help and his prolific suggestions. I am deeply grateful to him for his guidance, time, patience and support. I consider myself very fortunate for being able to work with a very considerate and encouraging professor like him.

Special thanks to Assoc. Prof. Abdulhadi Baykal, Zehra Durmuş and Tezcan Paralı for their contributions and all my colleagues.

My deepest gratitude goes to my husband for his unflagging love and support throughout my life.

My final words go to my family, most special thanks to my family, whose love and guidance is with me in whatever I persue, specially my very dear mum. I dedicate this thesis to my mum who unremittingly supported me during my years of study. She made this work possible.

TABLE OF CONTENTS

ABSTRACT…….iii
ÖZ…….iv
ACKNOWLEDGMENT……...v
TABLE OF CONTENTS…….....vi
LIST OF FIGURES……..ix
LIST OF ABBREVIATIONS.....xi
CHAPTER 1 INTRODUCTION..... 1
1.1 General Properties of Porphyrin..... 1
1.2 Physical and Chemical Properties of Porphyrin..... 2
1.2.1 Synthesis of Porphyrin……..5
1.3 Biologically Importance of Porphyrin..... 6
1.3.1 Biocompatibility of Porphyrin……...6
1.3.2 Cell-uptake Ability of Porphyrin…….. 8
CHAPTER 2 METAL NANOPARTICLES 9
2.1 Metal Nanoparticles. 9
2.2 Gold Nanoparticles..... 9
2.2.1 Gold Nanoparticles for Labelling……..……11
2.2.2 Gold Nanoparticles as a Vehicle for Delivery…….12
2.2.3 Hyperthermia effect of gold nanoparticles……..12
2.2.4 Gold Nanoparticles as Sensors……..……13
2.3 Porphyrin Capped Gold Nanoparticles 13
2.3.1 Gold (0) Porphyrins on Gold Nanoparticles…… .. 14
2.3.2 One-phase Synthesis of Small Gold Nanoparticles Coated by a Horizontal Porphyrin Monolayer…… …...16
2.3.3 Synthesis of Stably Water-Soluble Gold Nanoparticles Protected by Porphyrin-Thiol Derivative…….....19
CHAPTER 3 PHOTODYNAMIC THERAPY 21
3.1 Light Penetration Depth in PDT..... 21
3.2 Photophysical Process in PDT 22
3.2.1 Type I and Type II Mechanisms in PDT..... 24

3.3 General Remarks of Photosensitizers 24
CHAPTER 4 EXPERIMENTAL PART 27
4.1 CHEMICALS. 27
4.2 INSTRUMENTATION 27
4.3 EXPERIMENTAL PROCEDURE 28
4.3.1 One-pot synthesis of p-TPP-Sac 28
4.3.2 Synthesis of p-TPP-AuNPs 29
4.3.3 One-pot synthesis of m-TPP-Sac 29
4.3.4 Synthesis of m-TPP-AuNPs 30
4.3.5 One-pot synthesis of TBP-Sac 30
4.3.6 Synthesis of TBP-AuNPs 31
CHAPTER 5 RESULTS AND DISCUSSIONS 32
5.1 Spectral Characterization of p-TPP-SAc 32
5.2 Spectral Characterization of p-TPP-AuNPs 33
5.3 Spectral Characterization of m-TPP-SAc 37
5.4 Spectral Characterization of m-TPP-AuNPs. 39
5.5 Spectral Characterization of TBP-SAc 40
5.6 Spectral Characterization of TBP-AuNPs 41
CHAPTER 6 CONCLUSION 44
REFERENCES 45
APPENDIX A IR Spectrum of p-TPP 47
APPENDIX B IR Spectrum of p-TPP-SAc 48
APPENDIX C IR Spectrum of m-TPP 49
APPENDIX D IR Spectrum of m-TPP-SAc 50
APPENDIX E IR Spectrum of TBP 51
APPENDIX F IR Spectrum of TBP-SAc 52
APPENDIX G ^{1}H-NMR-Spectrum of p-TPP-SAc 53
APPENDIX H ^{1}H-NMR-Spectrum of m-TPP-SAc 54
APPENDIX I ^{1}H-NMR-Spectrum of TBP-SAc 55
APPENDIX J TEM image of p-TPP-AuNPs 56
APPENDIX K TEM image of m-TPP-AuNPs 57
APPENDIX L TEM image of TBP-AuNPs 58
APPENDIX M UV-vis. Spectra of p-TPP, p-TPP-Sac and p-TPP-AuNPs 59

APPENDIX N UV-vis. Spectra of m-TPP, m-TPP-Sac and m-TPP-AuNPs 60
APPENDIX O UV-vis. Spectrum of TBP-AuNPs 61
APPENDIX P Mass Spectra of p-TPP-SAc 62
APPENDIX R XRD Spectrum of p-TPP-AuNPs 63
APPENDIX S XPS Spectrum of p-TPP-AuNPs 64

LIST OF FIGURES

FIGURE

1.1 Porphine…….1
1.2 An example of Porphyrin……...1
1.3 Vitamin B12……...…2
1.4 UV-vis sectra of a porphyrin compound……3
1.5 Heme as a chelating agent……..4
1.6 An example of amphiphilic zinc porphyrin……4
1.7 Synthesis of porphyrin……5
1.8 Heme, Chlorophyll and vitamin B12, respectively 6
1.9 m-TPP and p-TPP, respectively 7
1.10 A bacteriochlorin derivative 7
2.1 AuNP coated by organic shells. 10
2.2 AuNP coated by organic shells 10
2.3 Gold Nanoparticle Surfaces by Bis (binaphthyl) Groups..... 11
2.4 AuNPs as a vehicle for delivery 12
2.5 AuNPs as a heat-source 13
2.6 SC_0P and SC_1P, respectively 14
2.7 TEM images of a) citrate- b) SC_0P-, and c) SC_1P-protected AuNPs. d) Schematic illustrations of the coordination of SCnP ligands on the Au surface……...15
2.8 UV/Vis spectra of a) SC_nP ligands and b) SC_nP-AuNPs 15
2.9 Structures of tetradentate and monodentate passivants, 1 and 2……..16
2.10 UV-Vis spectra of 1-AuNPs (red) and 1 (blue) in DMF……..17
2.11 TEM images of 1-AuNPs (a) and 2-AuNPs (b) 17
2.12 XPS spectra of S (2p) core level of 1-AuNPs (a) and 1 (b) and Au (4f) core level of 1-AuNPs (c) and 2-AuNPs (d) 18
2.13 Plausible structure of 1-AuNPs 19
2.14 TMP 19
2.15 TEM image and size distribution histogram of TMP-AuNPs, respectively….20
2.16 UV-vis spectra of TMP…….20

3.1 Phototherapeutic Window. 21
3.2 Jablonski Diagram 22
3.3 Ground, triplet and their excited states of a photosensitizer 23
3.4 Type I and Type II mechanisms 24
3.5 Schematic of tumor therapy using a photosensitizing drug and visible light incidence……...25
4.1 Synthesis of p-TPP-SAc. 28
4.2 Synthesis of m-TPP-SAc 30
4.3 Synthesis of TBP-SAc 31
5.1 ^{1}H-NMR-Spectrum of p-TPP-SAc 33
5.2 p-TPP (solid line), p-TPP-SAc (dotted line) and p-TPP-AuNPs (dashed line) 34
5.3 TEM image of p-TPP-AuNPs 34
5.4 XRD powder pattern and line profile fitting of p-TPP– AuNPs 35
5.5 XPS peaks of p-TPP-AuNPs for Au4f level 36
5.6 XPS peaks of p-TPP-AuNPs for S2s, S2p $_{3/2}$ and S2p$_{1/2}$ levels..... 36
5.7 XPS spectrum of p-TPP-AuNPs 37
5.8 p-TPP-AuNPs 37
5.9 ^{1}H-NMR-Spectrum of m-TPP-SAc 38
5.10 m-TPP (solid line), m-TPP-SAc (dotted line) and m-TPP-AuNPs (dashed line) 39
5.11 TEM image of m-TPP-AuNPs 40
5.12 m-TPP-AuNPs 40
5.13 ^{1}H-NMR-Spectrum of TBP-SAc 41
5.14 UV-vis. spectrum of TBP-AuNPs 42
5.15 TEM image of TBP-AuNPs 42
5.16 TBP-AuNPs 43

LIST OF ABBREVIATIONS

ABBREVIATION

p-TPP : meso-Tetra (p-hydroxyphenyl) porphyrin

p-TPP-SAc : Thiol-tailored meso-Tetra (p-hydroxyphenyl) porphyrin

p-TPP-AuNPs : meso-Tetra (p-hydroxyphenyl) porphyrin coated on gold nanoparticles

m-TPP : meso-Tetra (m-hydroxyphenyl) porphyrin

m-TPP-SAc : Thiol-tailored meso-Tetra (m-hydroxyphenyl) porphyrin

m-TPP-AuNPs : meso-Tetra (m-hydroxyphenyl) porphyrin coated on gold nanoparticles

TBP : 4-tert-butyl phenol

TBP-SAc : Thiol-tailored 4-tert-butyl phenol

TBP-AuNPs : 4-tert-butyl phenol coated on gold nanoparticles

TEA : Triethylamine

FT-IR : Fourier Transform Infrared

TEM : Transmission Electron Microscopy

NMR : Nuclear Magnetic Resonance

XPS : X-ray Photoelectron Spectroscopy

XRD : X-ray Diffraction Spectroscopy

CHAPTER 1

INTRODUCTION

1.1 General Properties of Porphyrin

Porphyrins are tetrapyrroles which many occur in nature. They are heterocyclic compounds characterised by four weakly aromatic pyrrole groups linked together by methine bridges (=CH-) which composed of both N atoms of pyrrole rings and two immino- hydrogen atoms in the center.

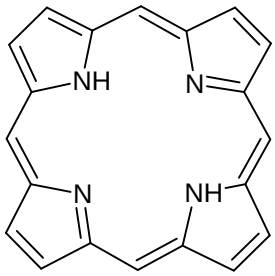

Figure 1.1 Porphine

The name of porphyrin is derived from the Greek word for purple. The simplest porphyrin is porphine, and derivated porphines are called porphyrins.

Porphyrins are a large family of related compounds that include the carbon-nitrogen framework presented in the figure 1.2.

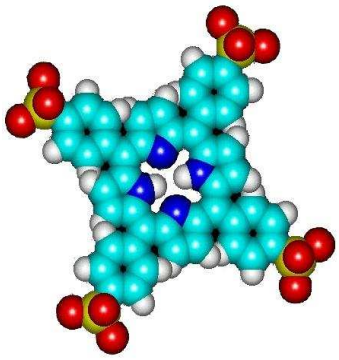

Figure 1.2 An example of Porphyrin [1]

The four nitrogen atoms on the center act as teeth, grabbing and holding metal ions such as cobalt (Co), iron (Fe) and magnesium (Mg).

They are extremely important organic compounds and have a vital process, especially when they grab some certain compounds. For instance, the vitamin B_{12} consists of a porphyrin molecule with a cobalt ion in the core.

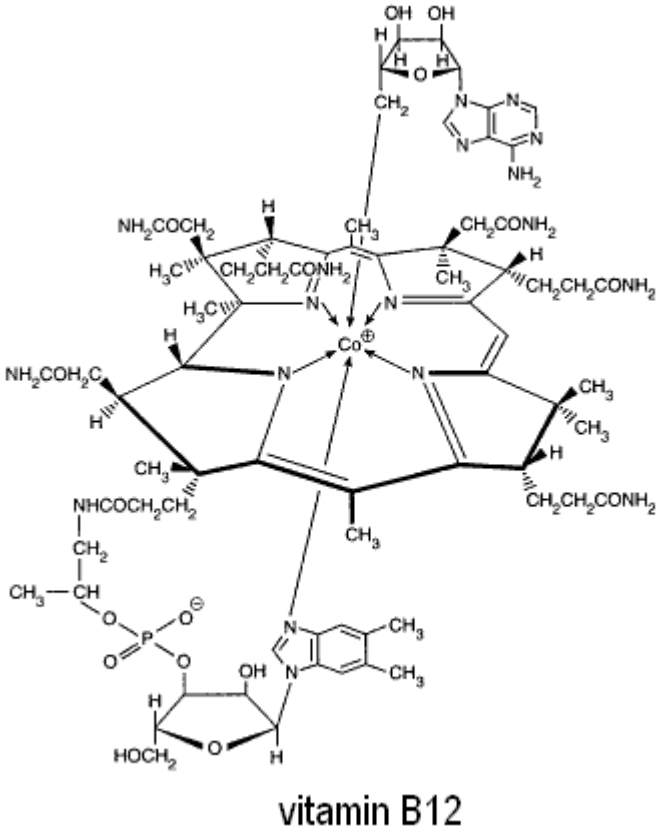

Figure 1.3 Vitamin B12 [2]

1.2 Physical and Chemical Properties of Porphyrin

The knowledge of the chemical and physical properties of porphyrins has grown rapidly, fuelling the expansion of research activities focused on the development of new synthetic methodologies and on the study of potential applications in optoelectronics, electrochemistry, catalysis, molecular recognition, sensors, data storage and solar cells. That is because porphyrins are related to the natural tetrapyrrolic macrocycles (e.g. chlorins, bacteriochlorins, porphyrinogens, and protoporphyrins), which feature a rigid planar aromatic organic ligand and a coordinated metal that introduces redox properties. These features permit

the natural tetrapyrrolic macrocycles and their synthetic homologues to play a central role in events such as electron transfer, oxygen transfer, and lightharvesting [3-7].

Porphyrins are aromatic, and they accord with the Hückel's rule for aromaticity. They possess 4n+2 π electrons (n=4 for the shortest cyclic path) that are delocalized over the macrocycle. That is the reason of macrocycles for having highly-conjugated systems and, as a consequence, porphyrins have very intense absorption in the visible region and thus, they are deeply colored, having a strong absorption band in the blue spectral range around 400 nm.

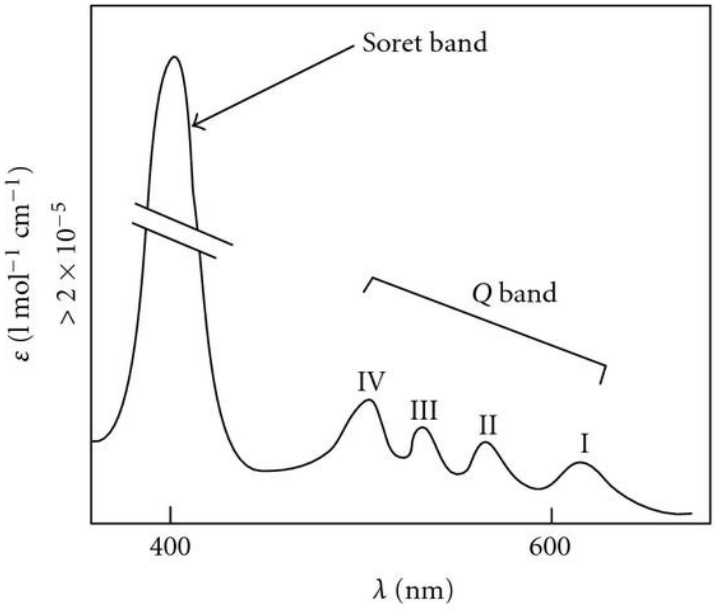

Figure 1.4 UV-vis spectrum of a porphyrin compound [8]

Porphine and its derivatives are unique chelating agents. A chelate is a chemical compound containing a metal ion attached by a chelating agent. Many biologically important chemicals are chelates. One of the most common example of a chelate is hemoglobin, which its complex molecule, heme has an iron (II) ion in the center, bonded to four nitrogen atoms with coordinate covalent bonds. As iron can form six bonds, four of these bonds come from porphyrin and each of two remaining bonds keep oxygen molecules as it is transported through the blood.

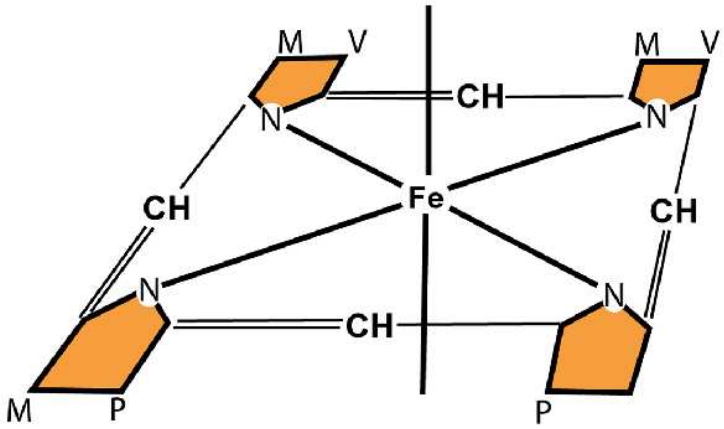

Figure 1.5 Heme as a chelating agent [9]

Also, they are readily derivatized, consenting with systematic studies and they do not aggregate extensively, simplifying analysis [10].

Porphyrins are amphiphilic organic compounds which have both hydrophilic and hydrophobic sides. Amphiphilicity is related to a molecule having a polar, water-soluble group bound to a non-polar water-insoluble hydrocarbon chain. It has been reported that amphiphilic photosensitizers are usually more photodynamically active than symmetrically hydrophobic or hydrophilic molecules [11-12].

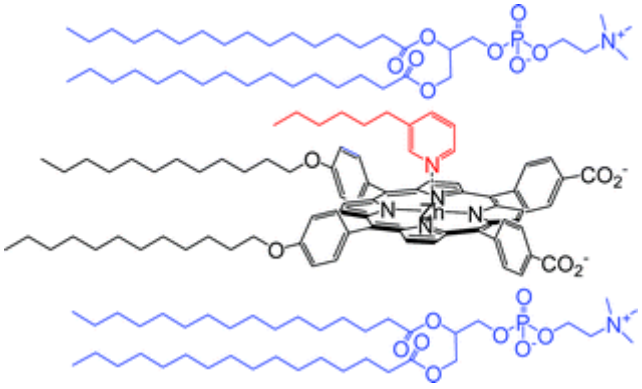

Figure 1.6 An example of amphiphilic zinc porphyrin [13]

The lipophilic side of a photosensitizer determines its localization and, therefore, the site of the cancerous cells. Lipophilic photosensitizers generally accumulate in the membrane of a cell and its organelles. On the other hand, the hydrophilic side, as well as agglomerated area of photosensitizers, penetrate into the cell by pynocitosis and are aggregated mainly in

lysosomes and endosomes. Maria and Julio had reported that the efficiency and selectivity of tumor targeting has been shown to increase slightly upon increasing the length of the alkyl groups [14].

Improving the efficiency of photodynamic therapy (PDT) is a quite popular research area. In PDT, the activation of a photosensitizer by light produces singlet molecular oxygen ($^1O_2$) which is highly active form of oxygen that reacts with many biomolecules, including lipids, proteins, and nucleic acids. The biomolecules are chemically modified by the action of $^1O_2$ and, thus, cannot accomplish their function, which leads to cell death [14].

1.2.1 Synthesis of Porphyrin

One of the most common synthesis for porphyrins is rooted in work by Paul Rothemund. His techniques give support to more modern synthesis such as those described by Adler and Longo. The synthesis of simple porphyrins such as meso-tetraphenylporphyrin (TPP) is also commonly synthesized in university teaching laboratories. It can be synthesized by heating an equally molar mixture of pyrrole and benzaldehyde in refluxing propionic acid for about an hour.

In this method, porphyrins are attained from pyrrole and substituted aldehydes. Acidic conditions are important; formic acid, acetic acid, and propionic acid are typical reaction solvents. A large amount of by-product is formed and is removed, usually by recrystallization or chromatography [15-18].

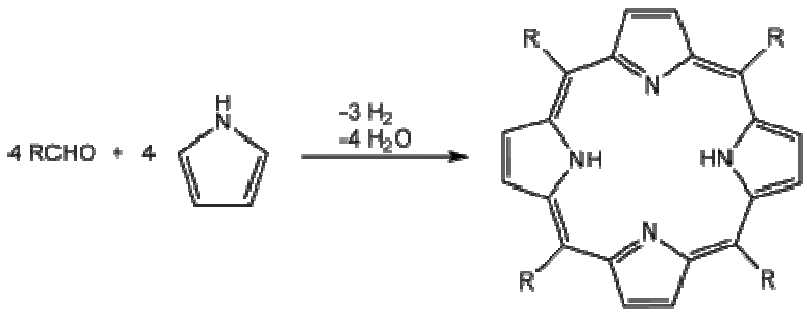

Figure 1.7 Synthesis of porphyrin [15-18]

1.3 Biologically Importance of Porphyrin

1.3.1 Biocompatibility of Porphyrin

Porphyrins are a class of biologically important heterocyclic compounds. They have a vital role in life process. Some biologically important porphyrins that take place in nature and in the human body are metal-centered porphyrins, for instance; Hemin-an iron porphyrin; Chlorophyll-magnesium porphyrin; vitamin B12-cobalt porphyrin [19]

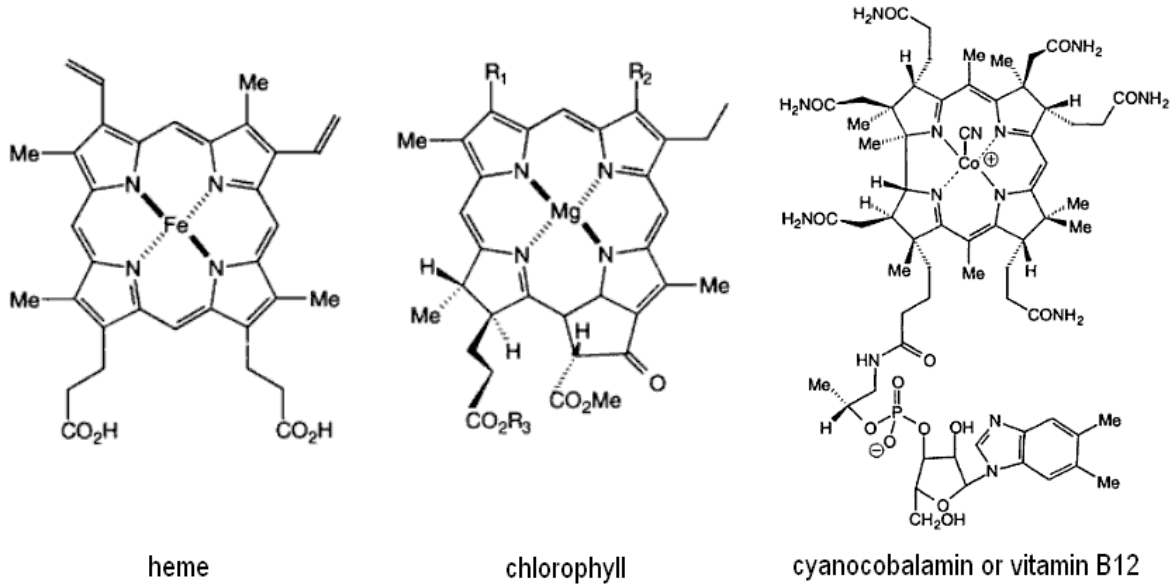

Figure 1.8 Heme, Chlorophyll and vitamin B12, respectively [2]

The thing is that porphyrins are capable to use in combination with almost any metal in the periodic table, so that this has drawn much attention by physical, organic, inorganic and biochemists.

Apart from metalloporphyrins, there have been several properties of porphyrins which attract chemist's attention, specifically their high stability due to having extention electronic conjugated structure, their high quantum yield, biocompatibility and cell-penetrating effect.

For instance, meso-tetra (m-hydroxyphenyl) porphyrin (m-TPP) and meso-tetra (p-hydroxyphenyl) porphyrin (p-TPP) show enhanced absorbtion in the red region. Also, they have useful tissue selectivity which is related to their amphiphilicity.

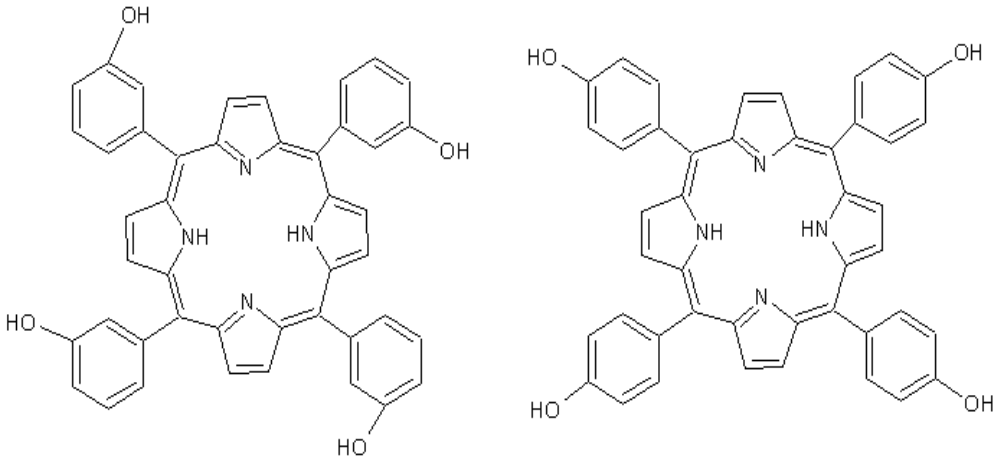

Figure 1.9 m-TPP and p-TPP, respectively

The reason of having a wide usage in biomedical fields of porphyrins is their biocompatibility. Several porphyrins with selected peripheral substitution and metal coordination carry out vital biochemical processes in living organisms. For instance, chlorins, bacteriochlorins, corphines and corrins, meso-tetra (m-hydoxy phenyl) porphyrins are related to tetra pyrrolic macrocycles that are also observed in biologically vital compounds.

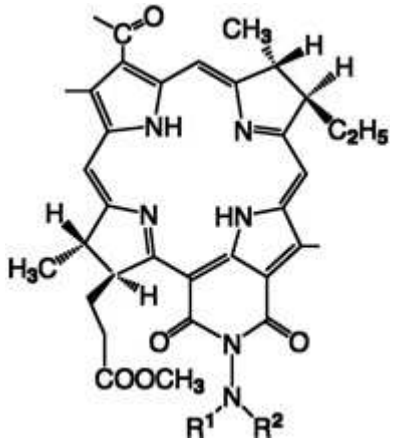

Figure 1.10 A bacteriochlorin derivative [20]

1.3.2 Cell-uptake Ability of Porphyrin

The cell-uptake ability of the component is essential concern as well as its biocompatibility. Cell uptake ability for a component is related to their chemical properties, size and hydrophilic – lipophilic character.

Porphyrins have a cell-penetrating ability [21]. For instance, m-TPP has been shown to be a very effective tumor photosensitizer in animal tumor models and in clinical trials. m-TPP-based PDT gives rise to a delay of the tumor growth. The peak values of the uptake of m-TPP by the tissues were found to decrease in the following order: spleen > urinary > tract > kidney > liver > lung > tumor > heart > skin > muscle > brain [22].

.

CHAPTER 2

METAL NANOPARTICLES

2.1 Metal Nanoparticles

Metal particles are nominately interesting nanoscale systems since they can be synthesized and modified chemically without difficulty.

Since metal nanoparticles are prone to come together, organic molecules, such citrate or sugar dextran, provide streric stabilization in order to prevent agglomeration. These stabilizers play essential role in protecting AuNPs [23].

There is a huge interest in metal nanoparticles, i.e. particles in the approximate size range 1 – 10 nm. These are applied in a variety of fields, the most important of which is catalysis. Industrial methods such as petroleum reforming depend on catalytic metal nanoparticles, as do the catalytic converters used to clean up motor vehicle exhausts. Metal nanoparticles are also applied in a range of other fields, including the labelling of biological samples, drug and gene delivery, tumor destruction via hyperthermia. The imperative part in this field is to make the particles as small as possible, with as narrow as possible a range of diameters. Transmission electron microscopy (TEM) is the main tool for this research [24].

2.2 Gold Nanoparticles

Organic molecules coated on metal nanoparticles, such as porphyrin, are relatively used in biomedical applications.

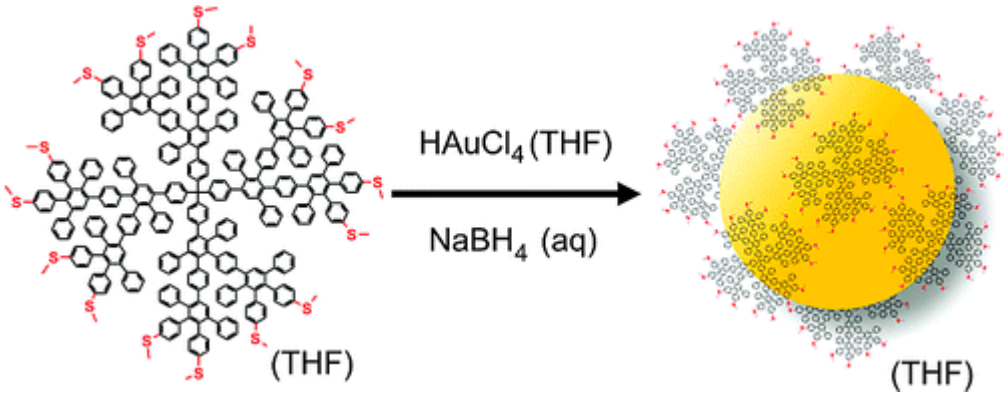

Figure 2.1 AuNP coated by organic shells [25]

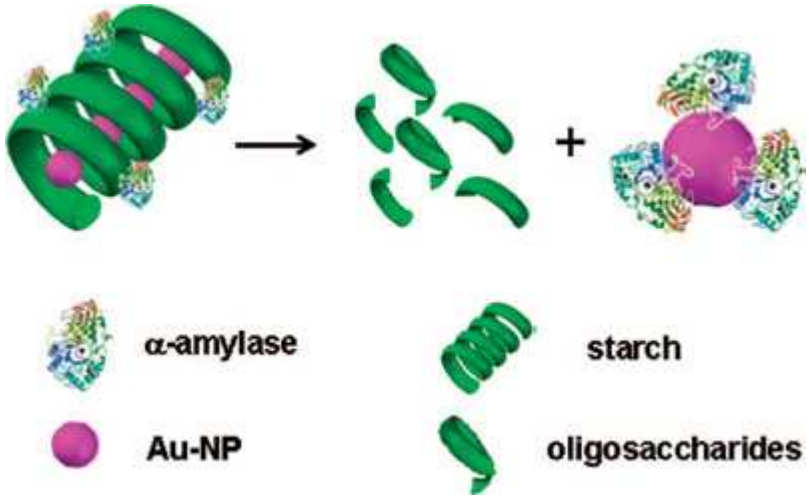

Figure 2.2 AuNP coated by organic shells [26]

Especially, AuNPs show unique optical properties due to localized surface plasmon oscillation in the visible region [27]. Thus, applications of surface plasmon oscillation of the AuNPs are quite interesting for excitation of organic molecules bound to the Au surface [28-29].

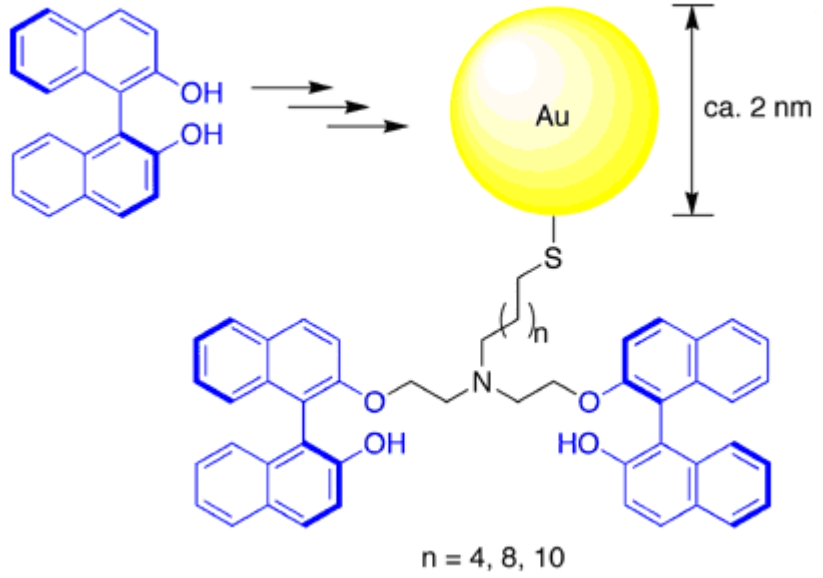

Figure 2.3 Gold Nanoparticle Surfaces by Bis (binaphthyl) Groups [30].

Organic molecules are assembled on the surface of AuNPs. The excitation of these organic molecules can be energy or charge transfer to oxygen molecule in the environment in a photodynamic process. The excited AuNPs also can act as energy donors to organic molecules so that the usual mechanism of fluorescence quenching of organic molecules by AuNPs is energy transfer.

Photoexcited AuNPs relax either nonradiatively [31] or by luminescence [32-33]. Nonradiative transitions are classified into two steps; internal conversion and intersystem crossing. Also, luminescence are classified into two steps, which are fluorescence and phosphorescence.

AuNPs are significantly categorized into four classes of applications in which have been used so far: labelling, delivering, heating and sensing [34].

2.2.1 Gold Nanoparticles for Labelling

AuNPs are a reasonably attractive contrast agent since they can be visualized with different techniques to detect each single particle level such as phase contrast/interference contrast microscopy, dark field microscopy, photothermal imaging, photoacoustic imaging, and fluorescence microscopy, XPS, TEM.

That is why; they are used as labels and make their conjugated molecules to be visualized under appropriate wavelength of light. Otherwise, the molecules of interest can not be differentiated from the other structures in the cells.

2.2.2 Gold Nanoparticles as a Vehicle for Delivery

Gold nanoparticles are used for delivery of molecules into cells. For this reason, the molecules are adsorbed on the surface of the Au particles and the whole conjugate is introduced into the cells. Inside cells the molecules will eventually separate themselves from the AuNPs [34].

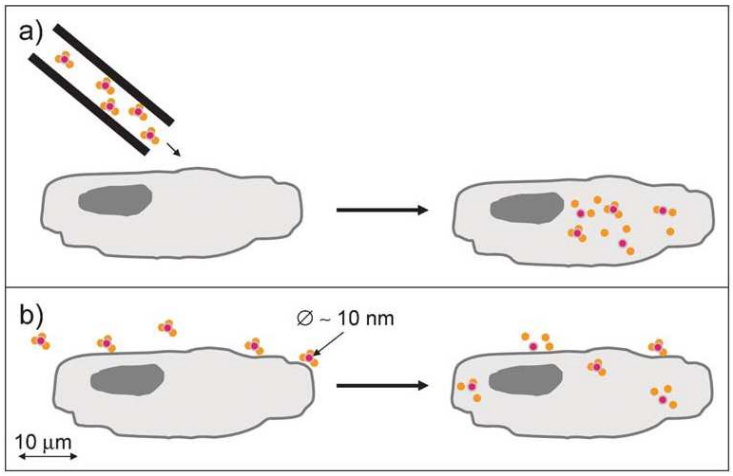

Figure 2.4 AuNPs as a vehicle for delivery [34].

2.2.3 Hyperthermia effect of gold nanoparticles

As mentioned above, when gold particles absorb light, the free electrons in the gold particles are excited. The excited electrons relax and the thermal energy is transferred to the lattice. Afterwards, the heat of the gold particles is dissipated into the surrounding environment, whereby the absorbed light energy is converted into thermal energy. Thus the idea is to enrich cancerous tissues with gold nanoparticles and to illuminate the tissue. Due to the heat mediated by the gold particles to the surrounding tissue, cancerous tissues can be destroyed locally without exposing the entire organism to elevated temperatures [34].

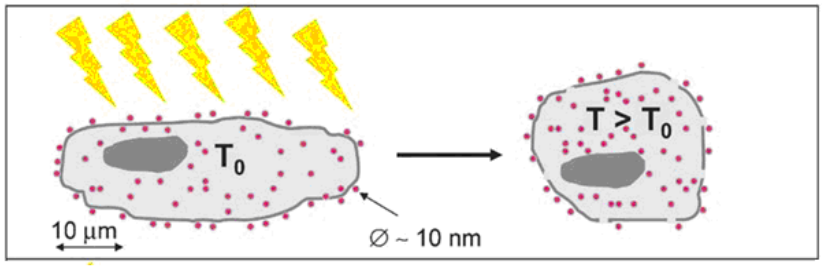

Figure 2.5 AuNPs as a heat-source [34]

Cells are very sensitive to even small increases in temperature. When temperature rises of a few degrees can give rise to cell death. Temperatures above 37^0C give rise to fever and above 42^0C are lethal for human beings. This fact can be used in a concept called hyperthermia. The key is to direct colloidal nanoparticles to the cancerous cells which can be done by conjugating the particle surface with ligands that are specific to receptors on cancer cells. The particles are then locally enriched in the cancerous [34].

2.2.4 Gold Nanoparticles as Sensors

The most popular detection techniques are rooted in the interaction between AuNPs and light. Gold particles strongly absorb and scatter visible light. When they are exposed to appropriate wavelength of light, the light energy excites the free electrons in the AuNPs. The excited electron acts as a donor and gives its excess energy to the acceptor molecule, so energy transfer occurs when AuNPs are used as sensors.

2.3 Porphyrin Capped Gold Nanoparticles

Recent studies have drawn much attention about the interaction between gold nanoparticles and pi-conjugated porphyrin systems.

Lately, it is been proved that multidentate passivants can enhance the stability of gold nanoparticles by testing a series of monodentate, bidentate and tridentate alkanethiols [35].

To have a better interaction between gold and porphyrin, thioester linkers are usually preferred, which contain sulphur atoms, exhibiting strong interaction with gold. For instance, meso-tetra (p-hydroxyphenyl) porphyrin and meso-tetra (m-hydroxyphenyl) porphyrin have been used as a protective ligand and modified by potassium thio acetate.

The key is that thioesters can easily dissociate to form S-Au bonds on gold surfaces. These groups are regarded an excellent thiol source to protect the Au surface [36].

There are some articles about porphyrin-gold interaction and its biological usage:

2.3.1 Gold (0) Porphyrins on Gold Nanoparticles [37]

AuNPs play important roles in different branches and especially have a wide usage in biomedical field. Many ligand-functionalized metal nanoparticles have been reported based on organic functional groups toward the nanoparticle surface to stabilize the nanoparticles.

Porphyrins are one of the most important p-conjugated compounds as organic functional groups for this purpose.

To attain stable AuNPs surrounded by p orbitals perpendicular to the Au surface, it had been focused on AuNPs formed through strong multidentate ligation using thiol derivatives.

Since the acetylthio groups easily dissociate to form S–Au bonds on bare Au surfaces, these groups are considered as an ideal source to protect the Au surface.

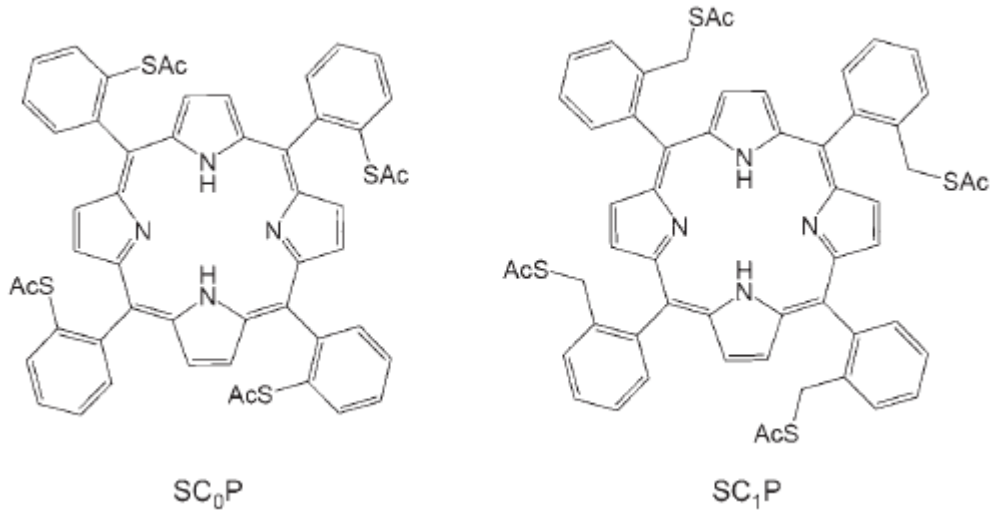

Figure 2.6 SC_0P and SC_1P, respectively [37]

As shown in Figure 2.7, tetrakis-5,10,15,20-(2-acetylthiophenyl) porphyrin (SC_0P) and tetrakis-5,10,15,20-(2-acetylthiomethylphenyl) porphyrin (SC_1P) had been synthesized. Thiol groups were used as linkers between the Au surface and the porphyrin ring in order to increase the distance between the porphyrin ring and the Au surface.

Porphyrin-protected AuNPs were prepared by ligand-exchange reaction from citrate-protected AuNPs.

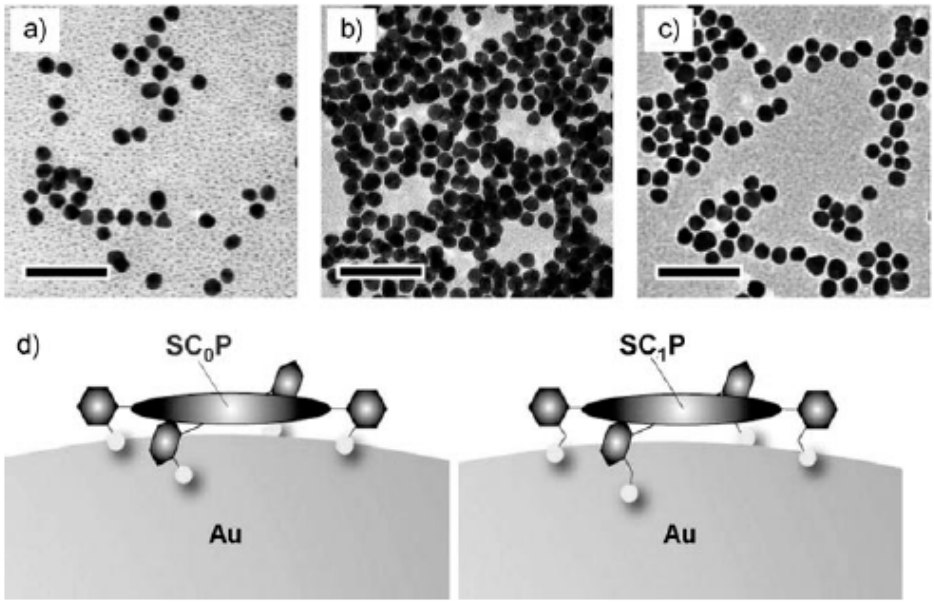

Figure 2.7 TEM images of a) citrate- b) SC_0P-, and c) SC_1P-protected AuNPs. d) Schematic illustrations of the coordination of SCnP ligands on the Au surface [37]

Figure 2.7 shows TEM images of the citrate-protected Au and porphyrin-protected AuNPs and no size change is observed.

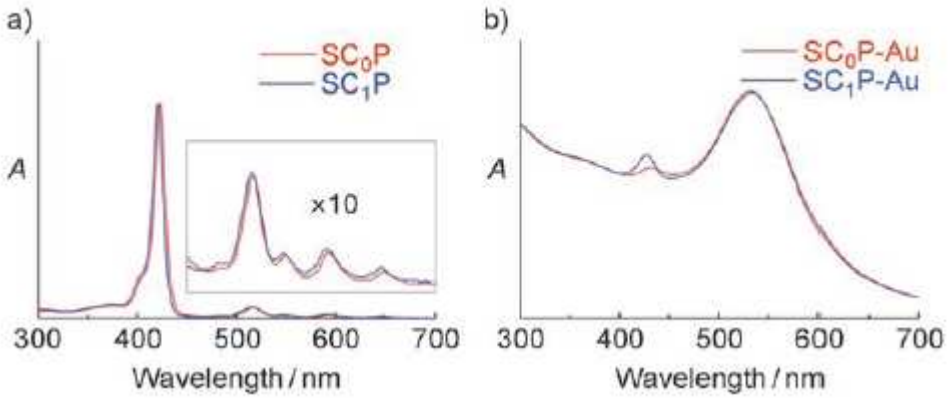

Figure 2.8 UV/Vis spectra of a) SC_nP ligands and b) SC_nP-AuNPs [37]

In the UV/Vis spectra, SC_0P and SC_1P gave Soret bands at 421 and 423 nm, respectively, and the SC_0P- and SC_1P-AuNPs were broadened and red-shifted to 432 and 427 nm, respectively, and four distinct Q bands in the range 515–646 nm. According to the coordination of the SC_nP ligands on the AuNPs, the Q bands for the SC_nP-AuNPs completely

disappeared, and the Soret bands for the SC_0P-Au and SC_1P-AuNPs were broadened and red-shifted to 432 and 427 nm, respectively. The drastic changes in the absorbance of the Soret band and Q band for SC_nP-AuNPs have to result from the change in electronic state of the porphyrins.

In conclusion, macrocyclic porphyrin ligands-protected AuNPs were synthesized. Considering the longer porphyrin–Au distance for SC_1P-Au, the interaction for SC_0P-Au is expected to be much larger than that for SC_1P-Au, resulting in the larger red-shift and the broadening of the Soret band for SC_0P-Au.

2.3.2 One-phase synthesis of small gold nanoparticles coated by a horizontal porphyrin monolayer [38]

Surface modification of AuNPs with functional molecules has been used as an ideal method to create nanoscale devices. It had been reported that porphyrin-cored tetradentate ligands by one-pot reduction of $HAuCl_4$, whose particle size is significantly smaller than that made by using monodentate passivants under identical conditions.

Horizontal porphyrin monolayer-coated AuNPs had been synthesized by a simple one-phase method; that is, the reduction of a $HAuCl_4$ solution containing multidentate ligands in order to evaluate the essential ability of the passivant ligand to produce and stabilize AuNPs without any assistance by other co-stabilizers such as citrate.

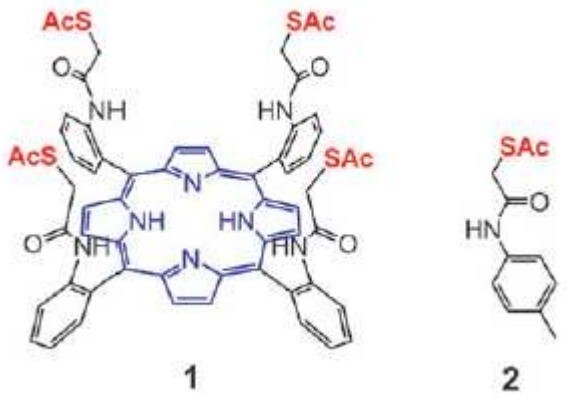

Figure 2.9 Structures of tetradentate and monodentate passivants, 1 and 2 [38]

Since all four sulfur atoms perpendicular to the porphyrin plane, they do not rotate away due to steric hindrance between the amide moiety and the porphyrin plane.

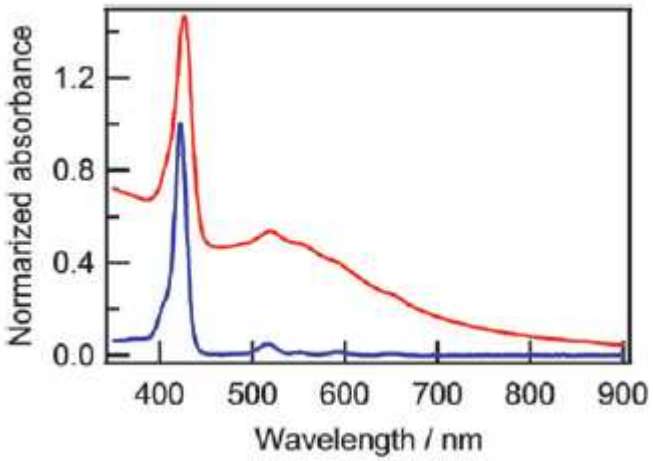

Figure 2.10 UV-Vis spectra of 1-AuNPs (red) and 1 (blue) in DMF [38]

Figure 2.10 shows UV-Vis spectra of 1 and AuNPs coated by 1 (1-AuNPs), indicating both characteristic bands of porphyrin and AuNPs at 426 nm and 500-670 nm, respectively.

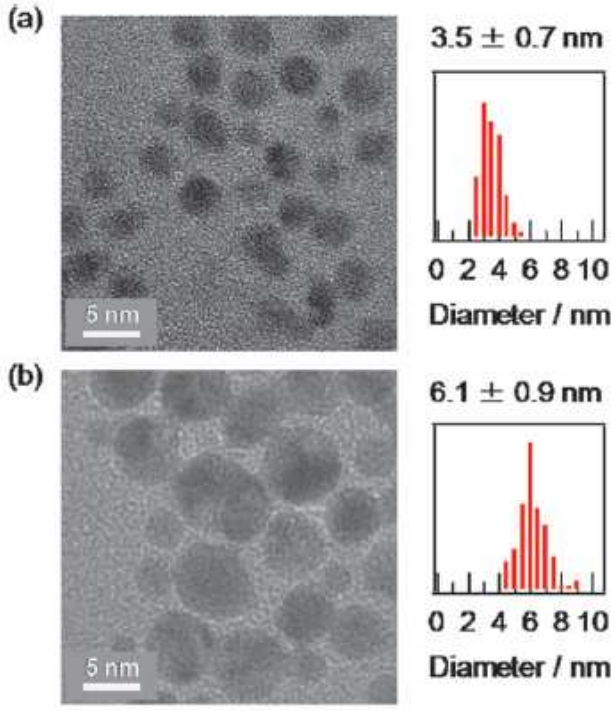

Figure 2.11 TEM images of 1-AuNPs (a) and 2-AuNPs (b) [38]

In the TEM image of the 1-AuNPs and 2-AuNPs, AuNPs are observed. Particle analysis revealed for 1-AuNPs, having a mean diameter of around 3.5 nm.

To control the size of 1-AuNPs, a monodentate-thiol-protected AuNPs (2-AuNPs) had been synthesized. The particle size of 2-AuNPs was larger than those of 1-AuNPs when compared at the same value of the ratio.

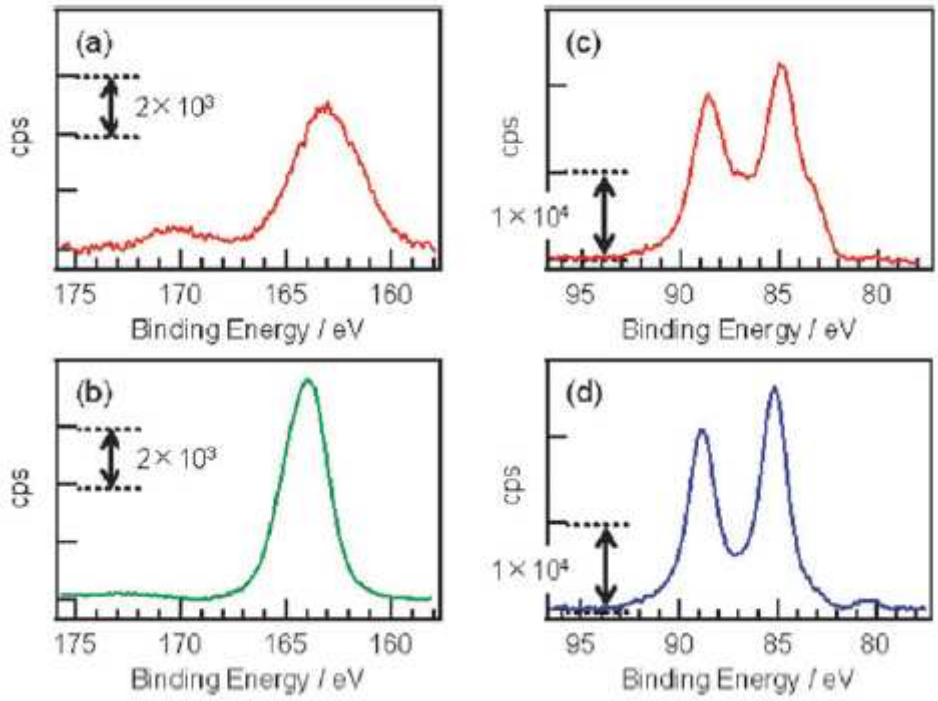

Figure 2.12 XPS spectra of S (2p) core level of 1-AuNPs (a) and 1 (b) and Au (4f) core level of 1-AuNPs (c) and 2-AuNPs (d) [38]

To detect the chemical status of 4 S atoms of 1-AuNPs, X-ray photoelectron spectroscopy was carried out. Figure 2.12 (a) shows the S (2p) measurement peaks at the binding energy of 163 eV, together with a very weak peak at 170 eV which is sulfur oxide coming from impurities derived from thiol-coated ligand. The main peak at 163 eV indicates the alkanethiol bound to Au. A similar spectrum is observed with 2-AuNPs.

These results indicated that thiol-coated porphyrin attached with the AuNP surface via four S-Au bonds.

Figure 2.12 (c, d) shows XPS spectra of Au (4f) core levels, which exhibits with a binding energy of 84.9 eV and 85.3 eV for 1-AuNPs and 2-AuNPs, respectively.

These results demonstrated that the gold cores of 1-AuNPs and 2-AuNPs were positively charged.

In conclusion, stable AuNPs coated by porphyrin monolayers by one-phase reduction of $HAuCl_4$ had been synthesized. This study indicated that highly functionalized multidentate passivants such as 1 control the size of AuNPs.

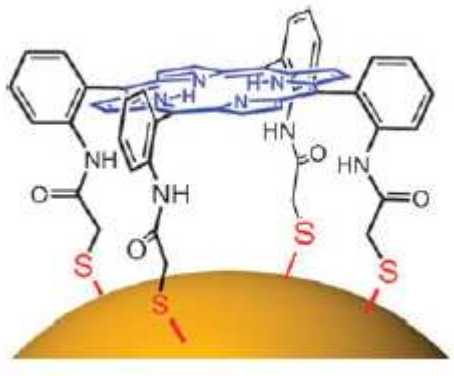

Figure 2.13 Plausible structure of 1-AuNPs [38]

2.3.3 Synthesis of Stably Water-Soluble Gold Nanoparticles Protected by Porphyrin-Thiol Derivative [39]

Masayuki and Toshiraru worked on water-soluble AuNPs coated by porphyrin. Thiol-tailored meso-tetra (3-mercaptophenyl) porphyrin (TMP) had been synthesized.

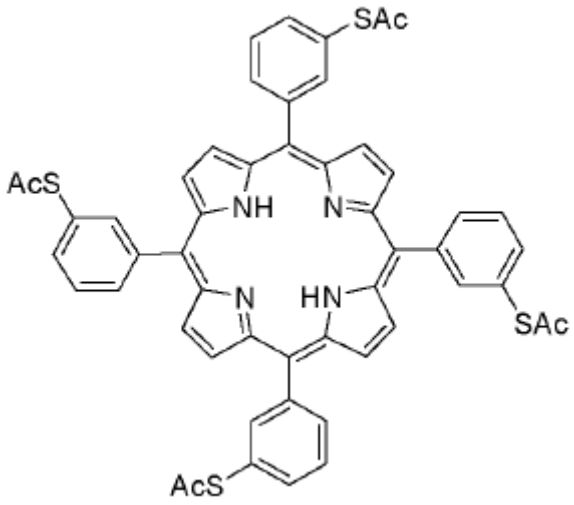

Figure 2.14 TMP [39]

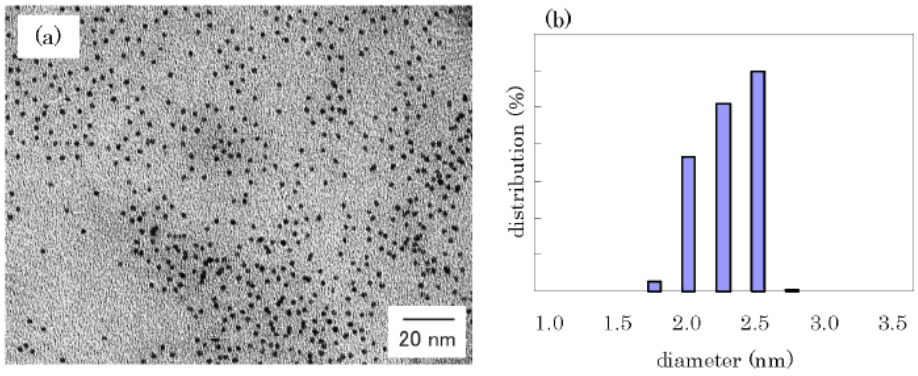

Figure 2.15 TEM image and size distribution histogram of TMP-AuNPs, respectively [39].

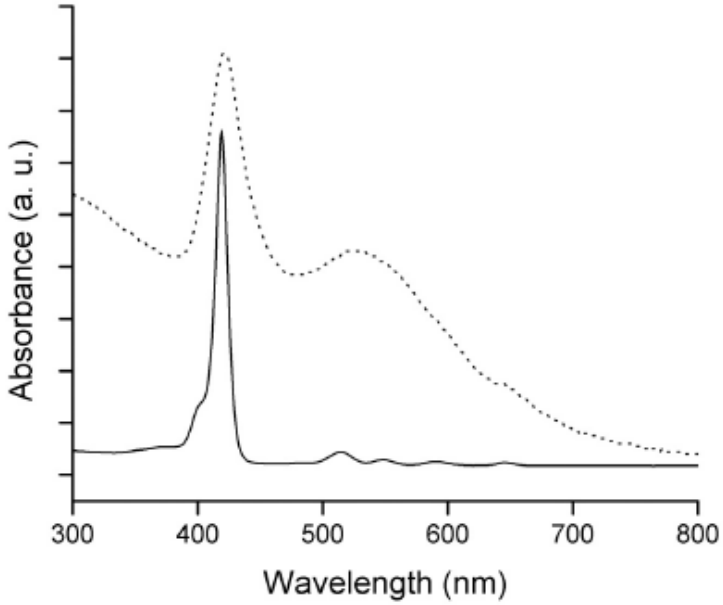

Figure 2.16 UV-vis spectra of TMP [39]

Figure 2.16 demonstrates that the UV-vis spectra containing TMP and Au ion (solid line) and TMP-AuNPs (dotted line). After the reduction of Au ion, the characteristic band of AuNPs had appeared around 520 nm.

The TEM image of TMP-AuNPs reports small AuNPs with very narrow size distribution, around 2.3 nm.

In conclusion, the highly stable TMP-AuNPs was obtained.

CHAPTER 3

PHOTODYNAMIC THERAPY

3.1 Light Penetration Depth in PDT

Light penetration depth is exceedingly related to the tissue type. However, the maximum of skin permeability occurs in the range of approximately 620-850 nm; light of the spectral range in the most tissues is around 600-700 nm which penetrates 50-200% deeper than light of the spectral range 400-500 nm [40].

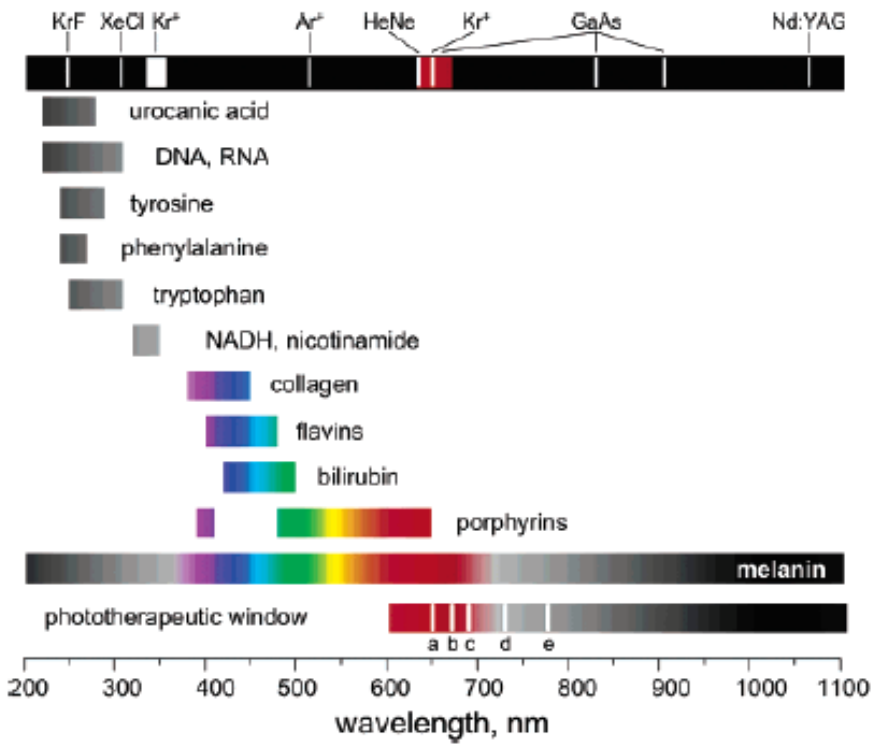

Figure 3.1 Phototherapeutic Window [40]

The spectral range above in figure 3.1 is called ‘‘Phototherapeutic Window’’ which is mostly used in photodynamic therapy.

3.2 Photophysical Process in PDT

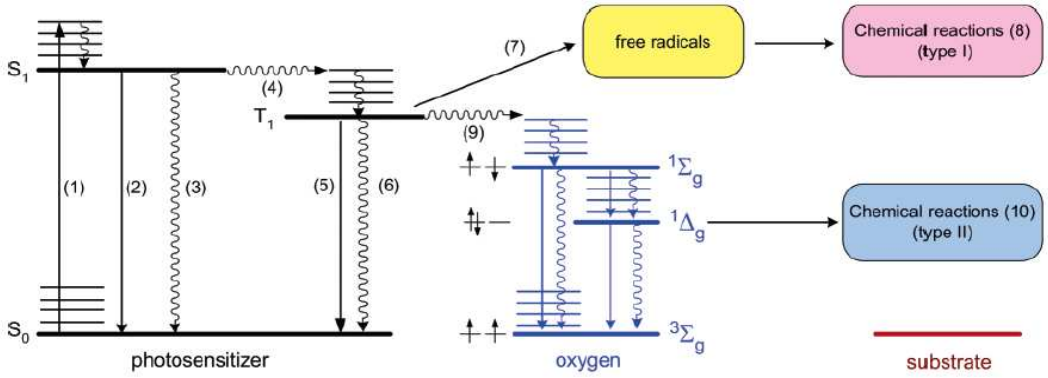

Figure 3.2 Jablonski Diagram [40]

Upon light absorption, a photosensitizer is excited from the electronic ground state (S_0) to a short-lived first excited singlet state (S_1) if there is no spin-change in the transition. If this electronic transition occurs by spin-change S_1 undergoes conversion to the first excited triplet state (T_1).

An excited photosensitizer is unstable and prone to go back to the ground state (S_0) by releasing its excess energy as light which is called luminescence (radiative transitions). Luminescence is categorized into two types: Fluorescence and Phosphorescence.

Florescence is defined when a photosensitizer returns to the S_0 state by emitting the absorbed energy. It takes place between the same states and usually occurs in the S_1 state. The lifetime of fluorescence is short (10^{-9}-10^{-5} s).

$$S_1 \rightarrow S_0 + h\nu$$

Phosphorescence is defined when a photosensitizer usually relaxes back by releasing energy from the T_1 state to the S_0 state. It takes place between the distinct states and its lifetime is short (10^{-3}-10^{-2} s).

$$T_1 \rightarrow S_0 + h\nu$$

T_1 state has lower energy than S_1 state, since two electrons have the same-routed spin. According to the Pauli principles, these same-routed spins cannot approach to each other so that there is a decrease in thrust between the spins. That is why; the system has lower energy than S_1 state which has distinct-routed spins.

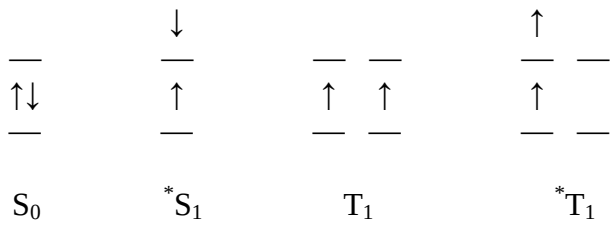

Figure 3.3 Ground, triplet and their excited states of a photosensitizer

In the figure 3.3 above, S_0, $^*S_1$, T_1, $^*T_1$ indicates ground state, the first excited state, triplet state and the first excited triplet state, respectively.

Alternatively, transition between the spins can take place by releasing heat. This system (non-radiative transitions) is categorized into two steps, as well: Internal Conversion (IC) and Intersystem Crossing (ISC).

Internal Conversion (IC) is defined when a photosensitizer returns to the S_0 state by releasing heat. This system occurs between the same states.

$$S_2 \rightarrow S_1 + \textit{heat}$$
$$T_2 \rightarrow T_1 + \textit{heat}$$
$$S_1 \rightarrow S_0 + \textit{heat}$$

Intersystem Crossing (ISC) is defined when a photosensitizer usually undergoes conversion from the S_1 state to the first excited triplet state by releasing heat (T_1).

$$S_1 \rightarrow T_1 + \textit{heat}$$
$$T_1 \rightarrow S_0 + \textit{heat}$$

The adequately long-lived T_1 state is able to take part in chemical reactions rooted in electron (or hydrogen) transfer (involved in photodynamic reactions of type I) and energy transfer (involved in photodynamic reactions of type II) [41].

3.2.1 Type I and Type II Mechanisms in PDT

Photosensitization takes place when an excited photosensitizer interacts with other molecules which could be oxygen, a solvent or a target molecule added to the solvent.

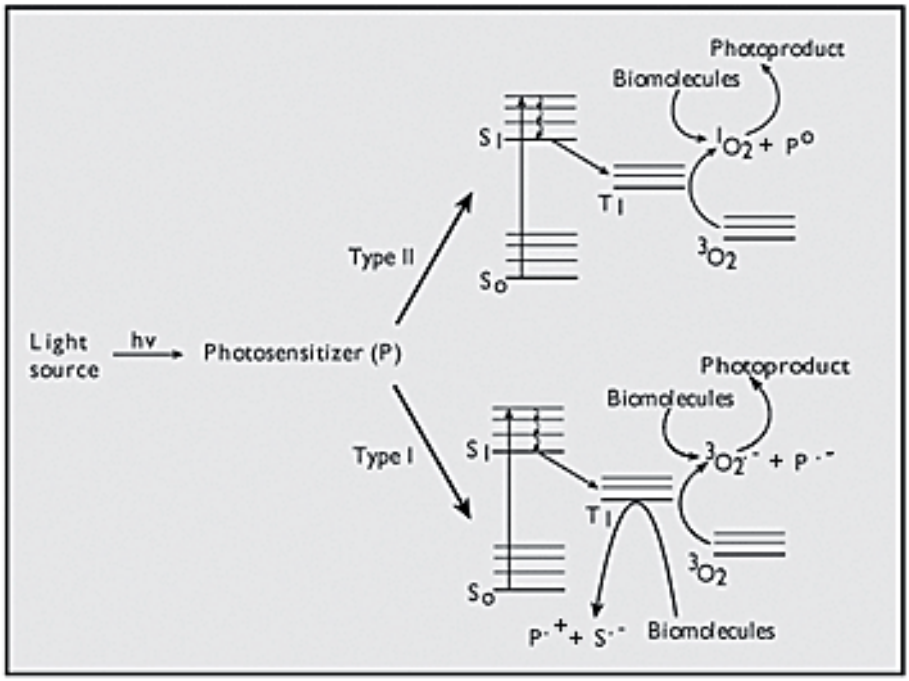

Figure 3.4 Type I and Type II mechanisms [42]

Photosensitized oxidation mechanisms are classified into two categories, called Type I and Type II photosensitization.

Type I photoreactions give rise to free-radical generation from a target molecule or the solvent.

Type II photoreactions produce chiefly reactive oxygen species and singlet oxygen which are extremely cytotoxic agents.

Nevertheless, the type II mechanism is mostly dominant due to the very reactive radicalic oxygen species.

That is to say, all charge-transfer reactions are classified as Type I photoreaction, whereas all energy-transfer reactions are classified as Type II photoreaction.

3.3 General Remarks of Photosensitizers

Photodynamic therapy is a quite new process for using in the central and healing of tumors by a photosensitizer, such as porphyrin, which localizes at, or near, the cancer cells, and when exposed to appropriate wavelength of light in the presence of oxygen to produce

radicalic materials, such as singlet oxygen ($^1O_2$). These chemicals are highly reactive form of oxygen that is produced by inverting the spin of one of the outermost electrons and can damage proteins, lipids, nucleic acids and other cellular components.

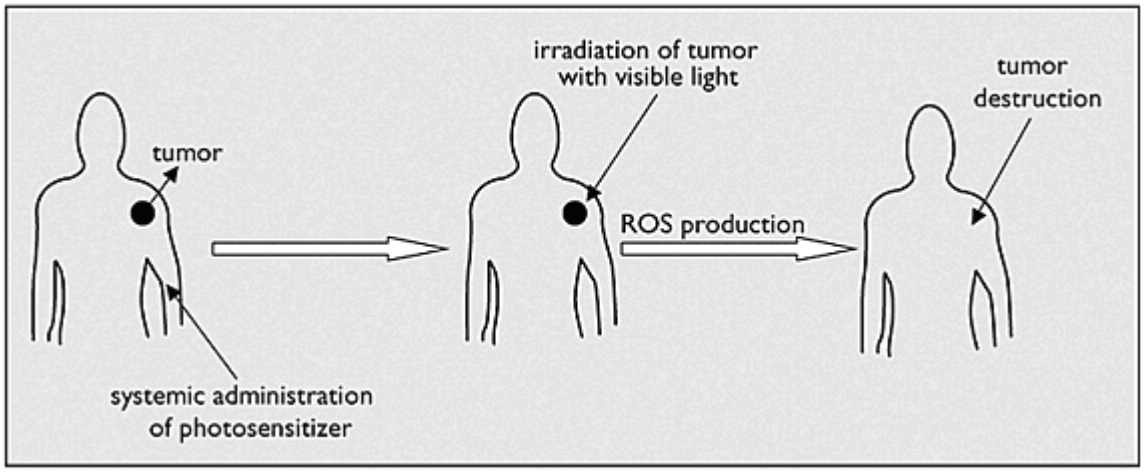

Figure 3.5 Schematic of tumor therapy using a photosensitizing drug and visible light incidence [42]

Basically, photosensitizers can absorb energy from photons (an appropriate wavelength of light) and transfer this energy to nearby oxygen molecules. As a result, toxic oxygen types, such as singlet oxygen and free radicals are formed.

Formation of cytotoxic species resulting from irradiation of a photosensitizer-loaded tumor is the most significant principle of PDT. This causes irrevocable damage to the neoplastic cells.

From the photophysical point of view, a good photosensitizer should have a high quantum yield of fluorescence for apparition of the tumor. It should engender singlet oxygen with a high quantum yield and /or easily accept (donate) electrons in its triplet state, this state should have an apposite energy and long enough lifetime to permit efficient energy or electron transfer to the oxygen molecule [43].

Presently, the most prevalently used photosensitizers are hematoporphyrin derivatives, phthalocyanines and synthetic porphyrins such as meso-tetraphenylporphyrin forms which are effective singlet oxygen generators [43].

Porphyrins demonstrate as an ideal photosensitizers since they are non-toxic, selectively retained in tumor tissue in high concentrations, cleared in a reasonable time from the body and swiftly from the skin which steer clear of photosensitive reaction.

In general, porphyrin and porphyrin-like compounds are prone to aggregate; causing a decrease of singlet oxygen generation and a reduction of the photosensitizing efficiency of a compound. The presence of additional ligands in the axial position obviously influences, both electronically and sterically, the environment of a metal complex. Additionally, if the ligand is hydrophilic, the solubility of the complex in aqueous phases is enhanced, which is important as the amphiphilic character of the photosensitizer is advantageous for PDT [39].

As photosensitizer, p-TPP and m-TPP are used due to having localized mainly in the stream of the tumors.

The high tumor sensitizing potency and convenient tissue selectivity of p-TPP and m-TPP make them encouraging nominees for clinical tumor phototherapy. It has been proved that p-TPP and m-TPP are highly effective tumor photosensitizers with interesting and possibly useful tissue selectivity [44].

CHAPTER 4

EXPERIMENTAL PART

4.1 CHEMICALS

meso-Tetra (p-hydroxy phenyl) porphyrin, meso-Tetra (m-hydroxy phenyl) porphyrin, 4- tert-butyl phenol, Bromoacetyl bromide, Potassium thio acetate, n- hexane, DMF, Ethanol, Methanol, Chloroform, Sodiumsulfate, Triethylamine, THF, $HAuCl_4$. H_2O, $NaBH_4$, piranha solution (H_2O_2: H_2SO_4).

4.2 INSTRUMENTATION

-Fourier Transform Infrared (FT-IR)

FT-IR spectra of some samples were recorded by Perkin Elmer FT-IR System, Spectrum BX, in the region 400-4000 cm^{-1}**.**

-UV Visible Spectroscopy

UV-visible spectra of the samples were recorded by UNICAM between the 300-800 nm.

-Transmission Electron Microscopy (TEM)

Transmission Electron Microscopy (TEM), analysis was performed using a FEI Tecnai G^2 Sphera Microscope.

-Nuclear Magnetic Resonance (NMR)

NMR studies of the samples were performed using a Bruker Ultra Shield Plus at a frequency of 400MHz.

-XRD

Huber JSO-DEBYEFLEX 1001 Diffractometer in GYTE, Philips diffractometer with PW 3020 goniometer and Rigaku diffractometer with D/max RINT-2200 with Cu K_α radiation were used for the characterization of p-TPP-AuNPs.

4.3 EXPERIMENTAL PROCEDURE

4.3.1 One-pot synthesis of p-TPP-SAc

A solution of p-TPP (0.2 g, 0.294 mole) in 32 mL dry THF was treated with TEA (244.30 µL, 1.764 mol) under N_2. Bromoacetyl bromide in 4.4 mL CH_2Cl_2 was added (306.96 µL, 3.528 mol) to the mixture dropwise over 10 min and stirred for 1 h at 0^0C.

Potassium thio acetate (0.671 g, 5.88 mole) in 10 mL absolute ethanol was added to the mixture and stirred for 2 h. The solvent was evaporated. The product was washed with water (15 mL) and n-hexane (15 mL) a few times and then taken into $CHCl_3$ (20 mL) phase. Standard workup and column chromatography of p-TPP-SAc (silica, $CHCl_3$/MeOH, 10:1) afforded a brown solid: ^{1}H-NMR ($CDCl_3$, 400 MHz): δ 2.564 (s, 12H), δ 4.153 (s, 8H), δ -2.819 (s, 2H), δ 8.239- δ 8.260 (dd, 8H), δ 7.561- δ 7.582 (dd, 8H), δ 8.893 (s, 8H); FT-IR C-O-C (1116 cm^{-1}), C=O (1740 cm^{-1}), S-C (1127 cm^{-1}), S-C=O (1690 cm^{-1}), $–CH_2$ and $–CH_3$ (3000-2800 cm^{-1}); UV-vis. (in $CHCl_3$): The Soret Band at 400 nm, four Q bands around 500-650 nm.

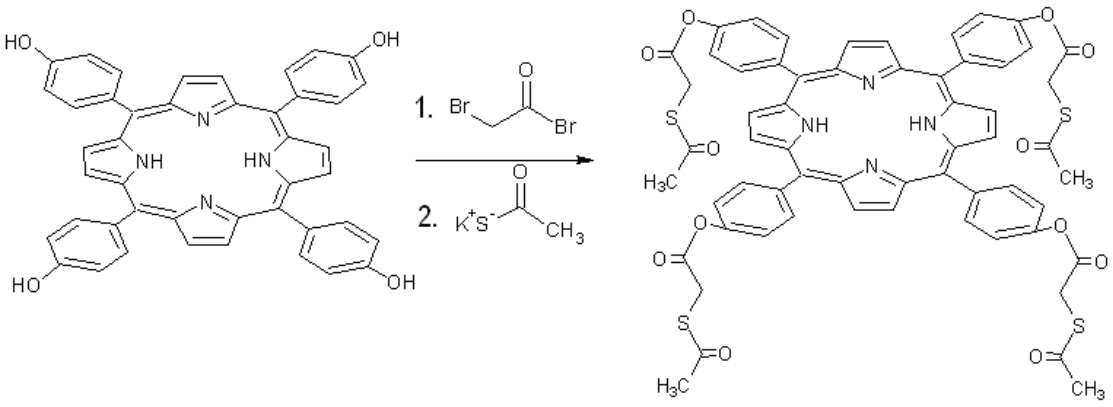

Figure 4.1 Synthesis of p-TPP-SAc

4.3.2 Synthesis of p-TPP-AuNPs

45.6 mg (0.04 mmole) thiol-tailored p-TPP in 250 mL DMF was added to a 500 mL round-bottom flask which has cleaned with piranha solution (a mixture of 3:1 concentrated sulfuric acid to 30% hydrogen peroxide solution). 112 mg (0.3 mmole) $HAuCl_4$ solution in 2 mL DMF was added to the mixture dropwise and the mixture was reduced with 73 mg $NaBH_4$ (in MeOH) by adding swiftly. The reaction mixture turned black straight away and was stirred at room temperature for 24 hours.

After 24 h stirring, the reaction mixture was evaporated to 3 mL. 40 mL of methanol was added to give a black precipitate which was collected by centrifugation. The precipitation process was repeated a few times and centrifuged in each stage. After that, the precipitate was deried under vacuum. Purified p-TPP-AuNPs was characterized by TEM, UV-vis, XRD and XPS measurements (See in Appendix J, M, R and S). UV-vis. (in MeOH): a characteristic broad peak of gold around 520 nm.

4.3.3 One-pot synthesis of m-TPP-SAc

A solution of m-TPP (0.2 g, 0.294 mole) in 32 mL dry THF was treated with TEA (244.30 μL, 1.764 mole) under N_2. Bromoacetyl bromide in 4.4 mL CH_2Cl_2 was added (306.96 μL, 3.528 mole) to the mixture dropwise over 10 min and stirred for 1 h at 0^0C.

Potassium thio acetate (0.671 g, 5.88 mole) in 10 mL absolute ethanol was added to the mixture and stirred for 2 h. The solvent was evaporated. The product was washed with water (15 mL) and n-hexane (15 mL) a few times and then taken into $CHCl_3$ (20 mL) phase. Standard workup and column chromatography of m-TPP-SAc (silica, $CHCl_3$/MeOH, 10:1) afforded a brown solid: ^{1}H-NMR ($CDCl_3$, 400 MHz): δ 2.459 (s, 12H), δ 4.047 (s, 8H), δ -2.884 (s, 2H, H_c), δ 7.450 (s, 4H), δ 7.952 (s, 4H), δ 7.993 (s, 4H), δ 8.014 (s, 4H), δ 8.804 (s, 8H)); FT-IR C-O-C (1128 cm^{-1}), C=O (1736 cm^{-1}), S-C (1154 cm^{-1}), S-C=O (1689 cm^{-1}), $–CH_2$ and $–CH_3$ (3000-2800 cm^{-1}); UV-vis. (in $CHCl_3$) The Soret Band at 400 nm, four Q bands around 500-650 nm.

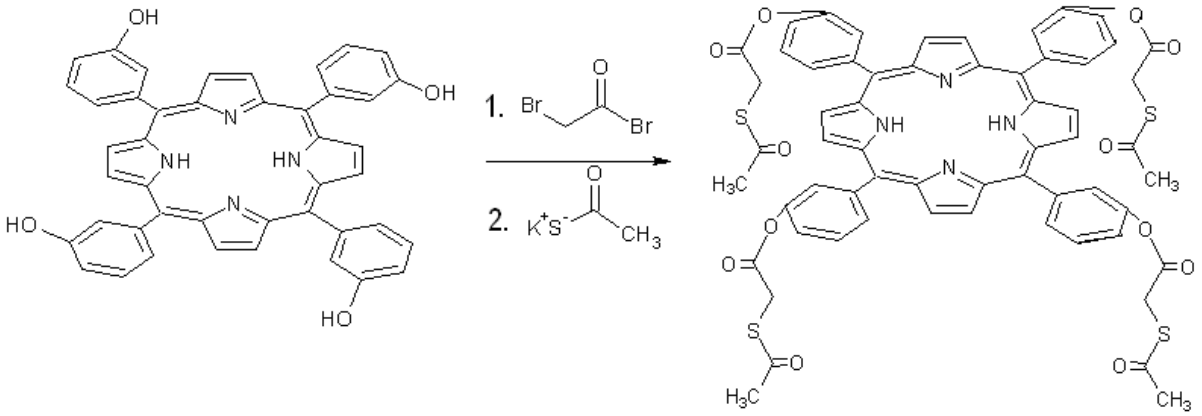

Figure 4.2 Synthesis of m-TPP-SAc

4.3.4 Synthesis of m-TPP-AuNPs

45.6 mg (0.04 mmole) thiol-tailored m-TPP in 250 mL DMF was added to a 500 mL round-bottom flask which has cleaned with piranha solution. 112 mg (0.3 mmole) $HAuCl_4$ solution in 2 mL DMF was added to the mixture dropwise and the mixture was reduced with 73 mg $NaBH_4$ (in MeOH) by adding swiftly. The reaction mixture turned deep brown straight away and was stirred at room temperature for 24 hours.

After 24 h stirring, the reaction mixture was evaporated. 40 mL of methanol was added to give a black precipitate which was collected by centrifugation. The precipitation process was repeated a few times and centrifuged in each stage. After that, the precipitate was deried under vacuum. Purified m-TPP-AuNPs was characterized by TEM and UV-vis measurements (See in Appendix K and N). UV-vis. (in MeOH): a characteristic broad peak of gold around 520 nm.

4.3.5 One-pot synthesis of TBP-SAc

A solution of 4-tert butyl phenol (0.3 g, 0.002 mole) in 32 mL dry THF was treated with TEA (415 μL, 0.003 mole) under N_2. Bromoacetyl bromide in 4.4 mL CH_2Cl_2 was added (435 μL, 0.005 mole) to the mixture dropwise over 10 min and stirred for 1 h at 0^0C.

Potassium thio acetate (0.158 g, 0.01 mole) in 10 mL absolute ethanol was added to the mixture and stirred for 2 h. The solvent was evaporated. The product was washed with water (15 mL) and n-hexane (15 mL) a few times and then taken into $CHCl_3$ (20 mL) phase. Standard workup and column chromatography of TBP-SAc (silica, $CHCl_3$/MeOH, 10:1) afforded a brown solid: ^{1}H-NMR ($CDCl_3$, 400 MHz): δ 1.240 (s, 9H), δ 2.358 (s, 13H), δ

3.852 (s, 2H), δ 7.299- δ 7.321 (dd, 2H), δ 6.945- δ 6.967 (dd, 2H); FT-IR C-O-C (1104 cm^{-1}), C=O (1738 cm^{-1}), S-C (1170 cm^{-1}), S-C=O (1696 cm^{-1}), $–CH_2$ and $–CH_3$ (3000-2800 cm^{-1}).

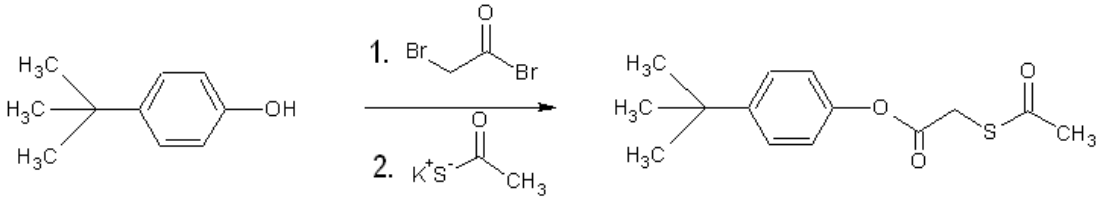

Figure 4.3 Synthesis of TBP-SAc

4.3.6 Synthesis of TBP-AuNPs

32 mg (0.12 mmole) thiol-tailored 4-tert butyl phenyl-SAc (TBP-SAc) in 250 mL DMF was added to a 500 mL round-bottom flask which has cleaned with piranha solution. 152 mg (0.45 mmole) $HAuCl_4$ solution in 2 mL DMF was added to the mixture dropwise and the mixture was reduced with 155.4 mg $NaBH_4$ (in MeOH) by adding swiftly. The reaction mixture turned dark yellow straight away and was stirred at room temperature for 24 hours.

After 24 h stirring, the reaction mixture was evaporated to 3 mL. 40 mL of methanol was added to give a black precipitate which was collected by centrifugation. The precipitation process was repeated a few times and centrifuged in each stage. After that, the precipitate was dried under vacuum. Purified TBP-AuNPs was characterized by TEM and UV-vis. Measurements (See in Appendix L and O). UV-vis. (in MeOH): a characteristic broad peak of gold around 520 nm.

CHAPTER 5

RESULTS AND DISCUSSIONS

5.1 Spectral Characterization of p-TPP-SAc

Thiol-tailored meso-tetra (p-hydroxyphenyl) porphyrin (p-TPP-SAc) had been successfully synthesized as an oily brown-coloured sample of the one-pot reaction between p-TPP, bromoacetyl bromide and potassium thio acetate in THF.

Firstly, p-TPP was activated with TEA, then bromoacetyl bromide was added which afforded the ester formation. After the washing of the crude product first with water and followed by n-hexane, the compound was taken into $CHCl_3$ phase and column chromatography (silica, $CHCl_3$/MeOH, 10:1) afforded an oily brown product.

In the IR spectrum of p-TPP-SAc, the characteristic C-O-C and C=O stretching ester groups, came out at 1127 cm^{-1} and 1740 cm^{-1}, respectively. Also, S-C and S-C=O stretching thio ester groups came out at 1116 cm^{-1} and 1690 cm^{-1}, respectively, as given in the literature for similar compounds. Disappearing of the –OH stretching groups at around 3600-3250 cm^{-1} and the peaks around 3000-2800 cm^{-1} indicated $–CH_2$ and $–CH_3$ aliphatic stretching groups of p-TPP-SAc.

In the ^{1}H-NMR spectrum of p-TPP-SAc, the chemical shifts at 2.56 ppm, 4.15 ppm and -2.82 ppm can be attributed to $OC-CH_3$, $OC-CH_2$-S- and HN- groups, respectively. In addition, the protons of aromatic rings of porphyrin macrocycle (d and e) were observed at 7.58 (doublet) ppm and 8.26 (doublet) ppm, respectively. Also, the HC- protons of the porphyrin ring were observed at 8.89 ppm (Fig. 5.1).

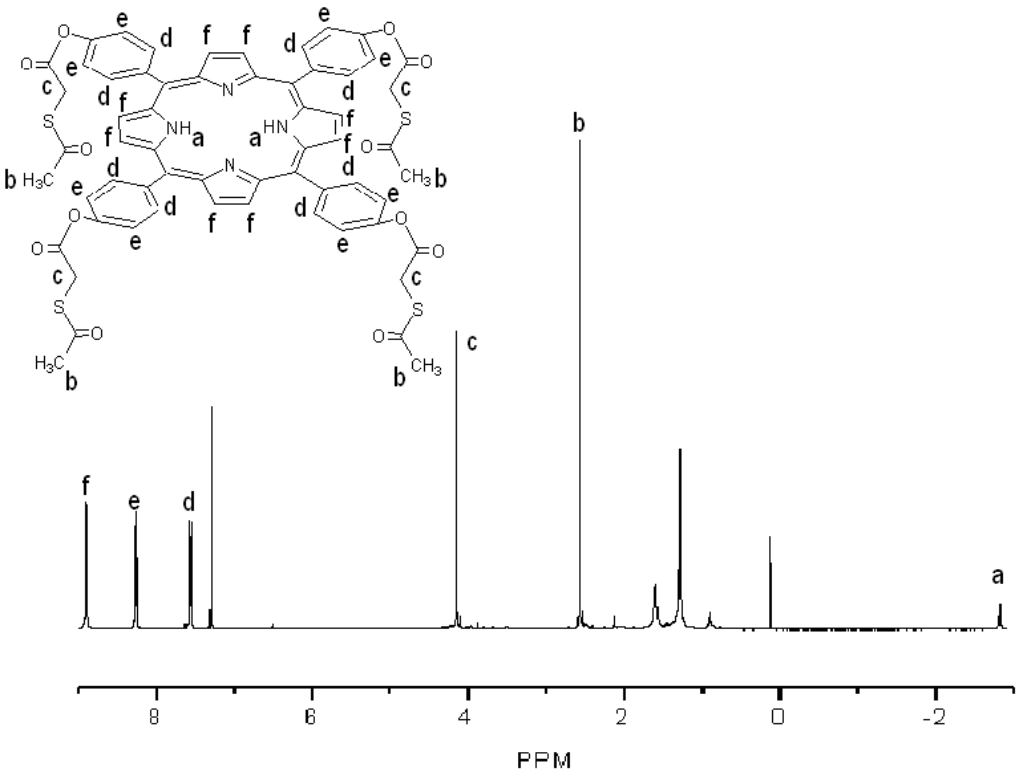

Figure 5.1 ^{1}H-NMR-Spectrum of p-TPP-SAc

After the formation of p-TPP-SAc, the colour of p-TPP turned from purple to brown. This was followed by UV-vis spectrum (Fig. 5.2). The two of the characteristic peaks of p-TPP at around 400 nm and 520 nm shifted to the shorter wavelength by about 5 nm which is most probably the result of the phenolic ester formation, indicating no change in the electron density of the porphyrin skeleton.

In the LC- MS spectrum (See Appendix P) of p-TPP-SAc, the molecular ion peak can be observed at 1143.725 m/z which shows that the four phenyl groups of the p-TPP interacted with –SAc.

5.2 Spectral Characterization of p-TPP-AuNPs

p-TPP-SAc was then coated on AuNPs in the presence of $HAuCl_4$ and $NaBH_4$ in DMF solution.

The newly-synthesized compound (p-TPP-AuNPs) was characterized by UV-vis. spectrum in which the broad peak around 520 nm indicates the formation of AuNPs (Fig. 5.2).

In the TEM image, the dark-coloured nanoparticles show the porphyrin coated on AuNPs.

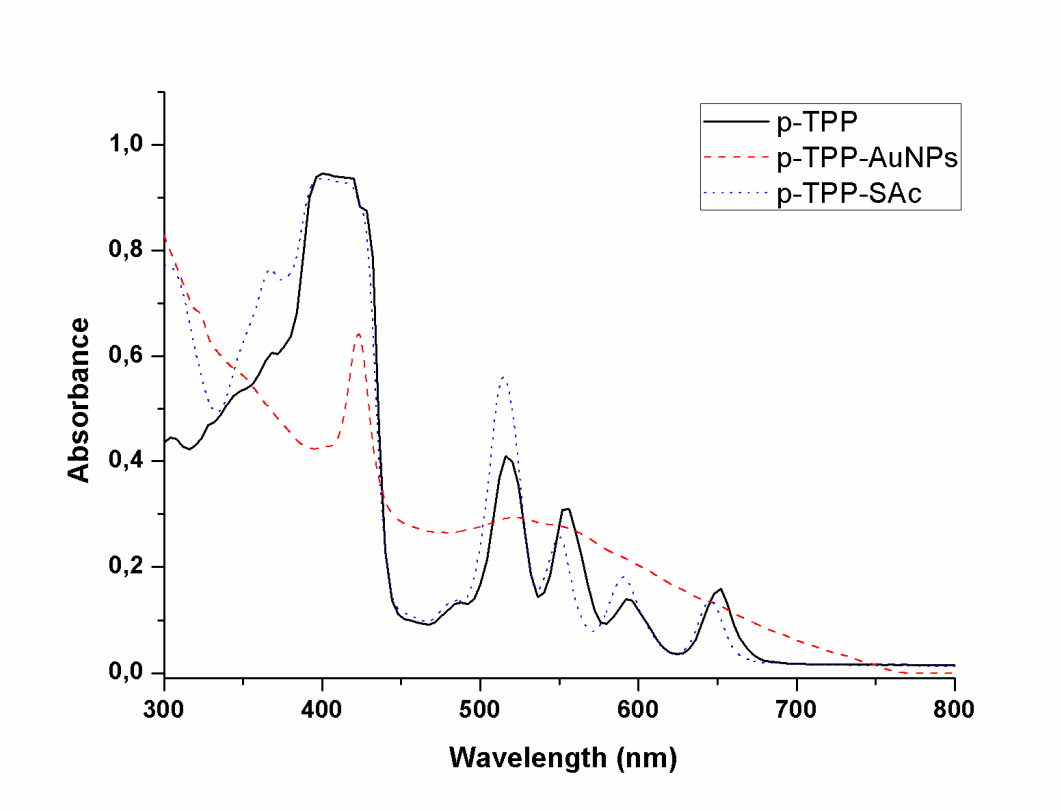

Figure 5.2 p-TPP (solid line), p-TPP-SAc (dotted line) and p-TPP-AuNPs (dashed line)

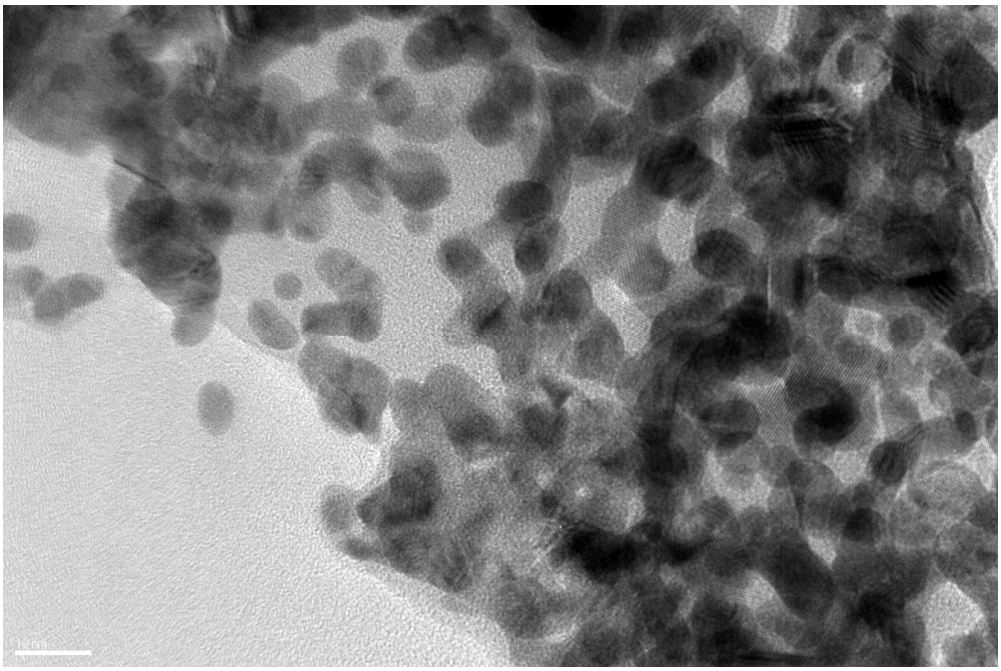

Figure 5.3 TEM image of p-TPP-AuNPs

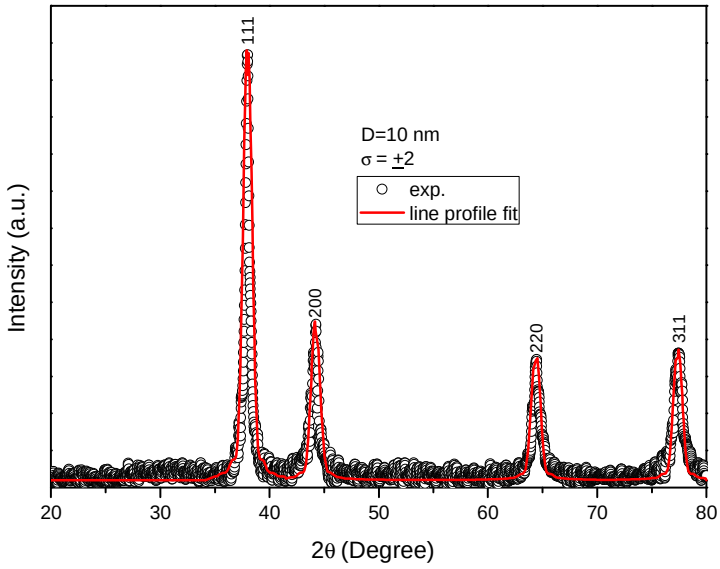

Figure 5.4 XRD powder pattern and line profile fitting of p-TPP-AuNPs

Phase investigation of the as-synthesized powder was performed by XRD and the diffraction pattern is presented in Fig.5.4. The XRD pattern indicates that the product consists of Au, and the diffraction peaks are broadened owing to very small crystallite size. All of the observed diffraction peaks are indexed by the cubic structure of Gold (JCPDS no. 04-0784) revealing a high phase purity of product [45-46]. There is some amorphous component causing a high background at low angles –up to 20^{o}- in the XRD pattern, which could be due to the presence of the p-TPP-AuNPs. The mean size of the crystallites was estimated from the diffraction pattern by line profile fitting method described in Ref 45 and 46. The line profile indicated by a continuous line, shown in Fig. 5.4, was fitted for observed four peaks with the following miller indices: (111), (200), (220), and (311). The average crystallite size, D and σ, was obtained as 10 ±2 nm as a result of this line profile fitting.

Alkanethiol molecules are competent for adsorbing onto Au surface through Au–S bonding and self-assemble into an ordered structure at the molecular scale called a self-assembled monolayer (SAM). XPS was used to characterize the oxidation state of Au in the NPs [47]. The binding energy (BE) scales were referenced to the Au $4f_{7/2}$ level at 85.0 eV [48] and to the S2p $_{3/2}$ and $S2p_{1/2}$ levels at about 168 eV (with 2:1 ratio of photo-ionization cross sections, which the peaks were assumed to have the same width, identifying each doublet in terms of the position of the 3/2 peak) [49]. As these references are taken into account, the

XPS results of p-TPP-SAc showed similar peaks for Au4f (84 eV) and S2p (S2p $_{3/2}$ and S2p$_{1/2}$ levels at about 164 eV and 170 eV, respectively) levels.

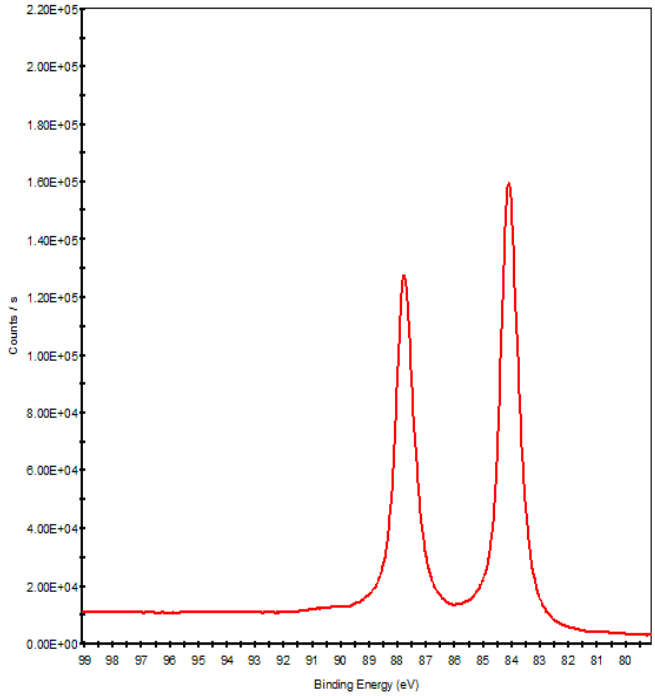

Figure 5.5 XPS peaks of p-TPP-AuNPs for Au4f level

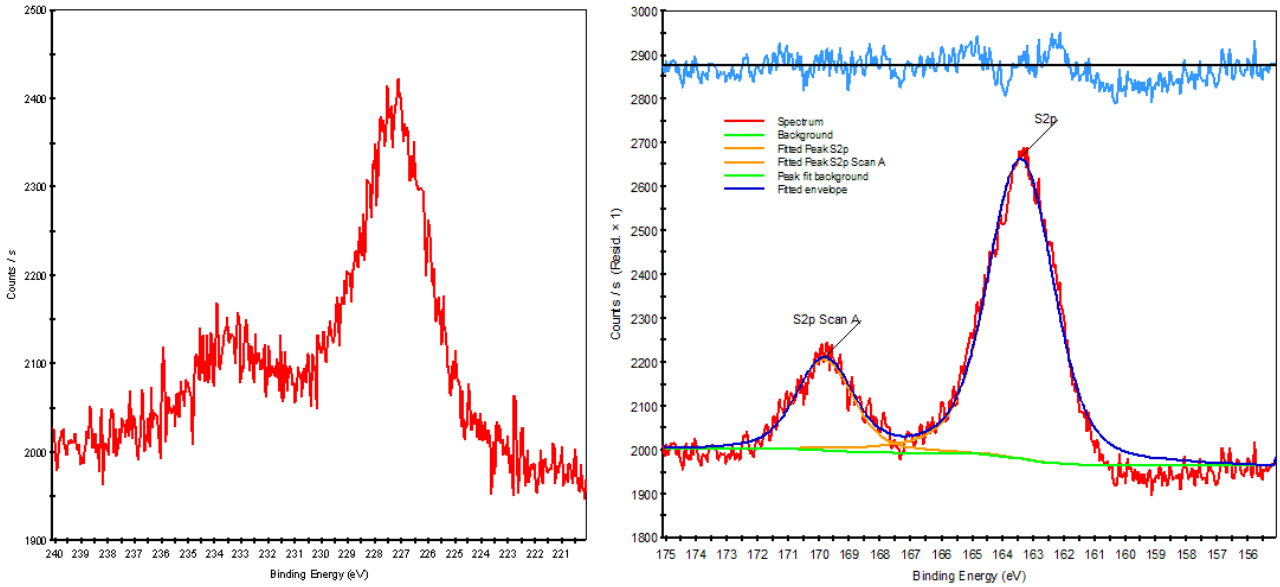

Figure 5.6 XPS peaks of p-TPP-AuNPs for S2s, S2p $_{3/2}$ and S2p$_{1/2}$ levels

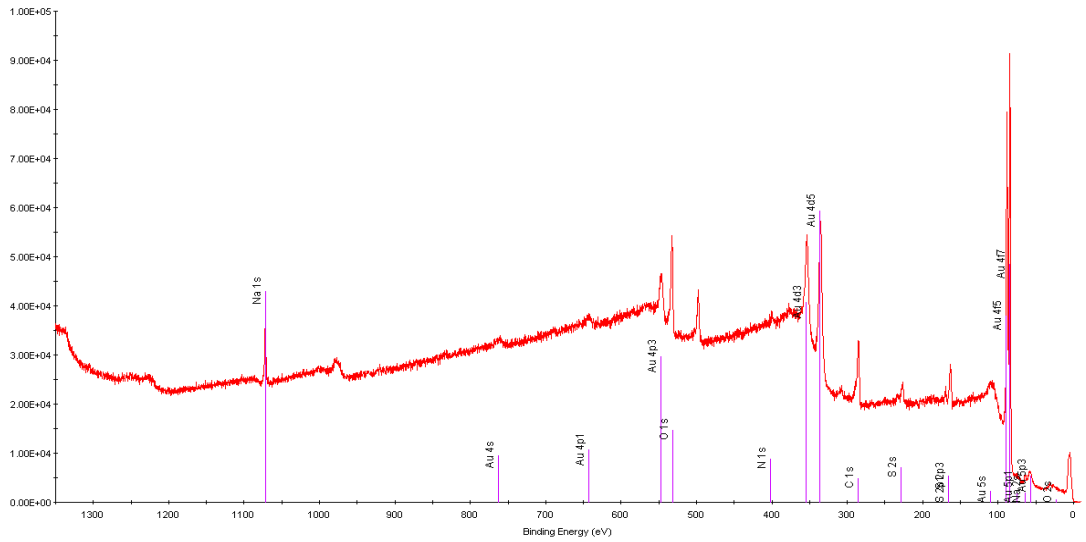

Figure 5.7 XPS spectrum of p-TPP-AuNPs

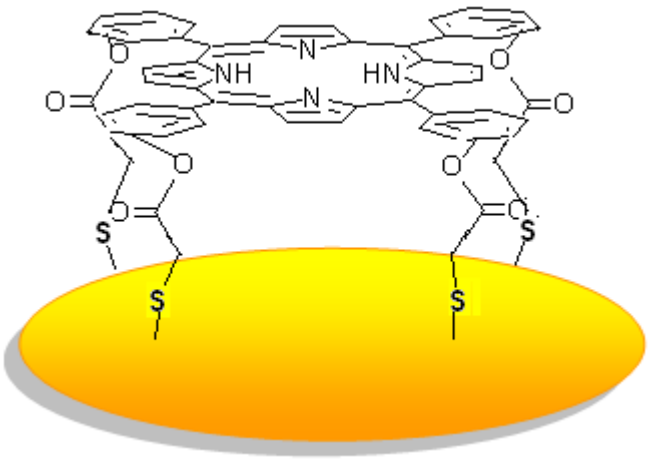

Figure 5.8 p-TPP-AuNPs

5.3 Spectral Characterization of m-TPP-SAc

Thiol-tailored meso-tetra (p-hydroxyphenyl) porphyrin (m-TPP-SAc) had been successfully synthesized as an oily brown-coloured sample of the one-pot reaction between m-TPP, bromoacetyl bromide and potassium thio acetate in THF.

Firstly, m-TPP was activated with TEA, then bromoacetyl bromide was added which afforded the ester formation. After the washing of the crude product first with water and followed by n-hexane, the compound was taken into $CHCl_3$ phase and column chromatography (silica, $CHCl_3$/MeOH, 10:1) afforded an oily brown product.

In the IR spectrum of m-TPP-SAc, characteristic C-O-C and C=O stretching ester groups, came out at 1154 cm^{-1} and 1736 cm^{-1}, respectively. Also, S-C and S-C=O stretching thio ester groups came out at 1128 cm^{-1} and 1689 cm^{-1}, respectively, as given in the literature for similar compounds. Disappearing of the –OH stretching groups at around 3600-3250 cm^{-1} and the peaks around 3000-2800 cm^{-1} indicated $–CH_2$ and $–CH_3$ aliphatic stretching groups of m-TPP-SAc.

In the ^{1}H-NMR spectrum of m-TPP-SAc, the chemical shifts at 2.46 ppm, 4.05 ppm and -2.88 ppm can be attributed to $OC-CH_3$, $OC-CH_2$-S- and HN- groups, respectively. In addition, the protons of aromatic rings of porphyrin macrocycle (d, e, f and g) were observed at 7.45 ppm, 7.95 ppm, 7.99 ppm and 8.01 ppm, respectively. Also, the HC- protons of the porphyrin ring were observed at 8.80 ppm.

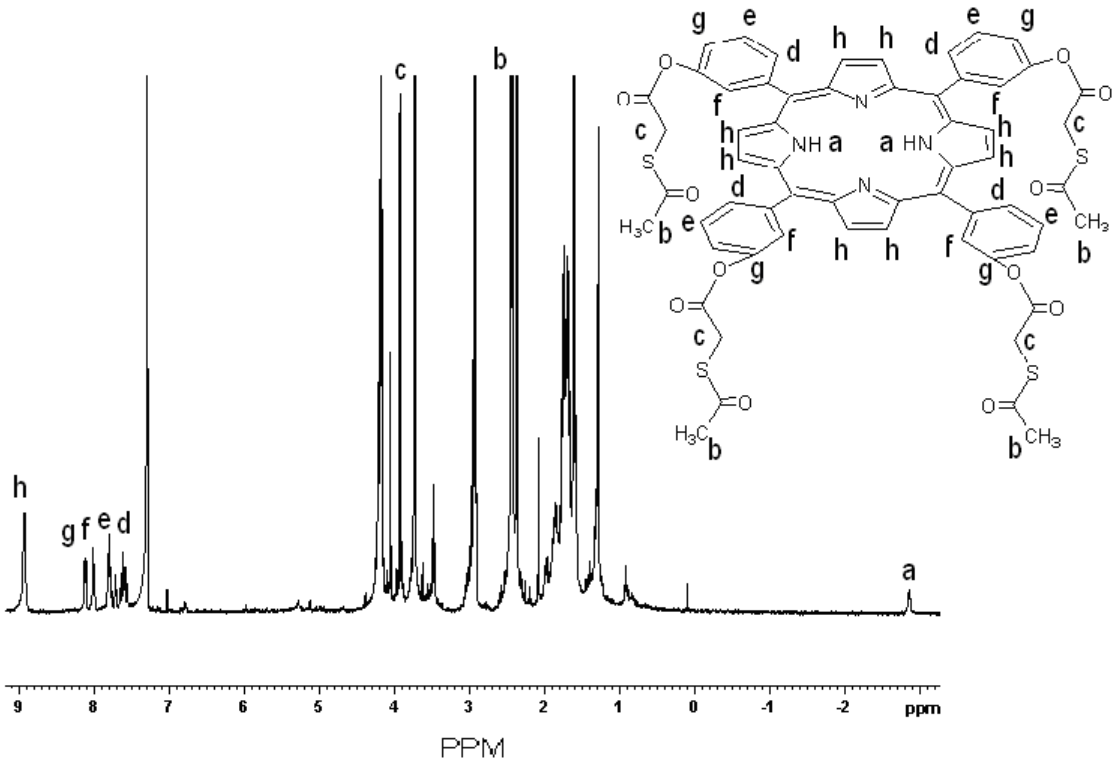

Figure 5.9 ^{1}H-NMR-Spectrum of m-TPP-SAc

After the formation of m-TPP-SAc, the colour of m-TPP turned from purple to brown. This was followed by UV-vis spectrum (Fig. 5.9). The two of the characteristic peaks of p-

TPP at around 400 nm and 520 nm shifted to the shorter wavelength by about 5 nm which is most probably the result of the phenolic ester formation, indicating no change in the electron density of the porphyrin skeleton.

5.4 Spectral Characterization of m-TPP-AuNPs

m-TPP-SAc was then coated on AuNPs in the presence of $HAuCl_4$ and $NaBH_4$ in DMF solution.

The newly-synthesized compound (m-TPP-AuNPs) was characterized by UV-vis. spectrum in which the broad peak around 520 nm indicates the formation of AuNPs (Fig. 5.10).

In the TEM image, the dark-coloured nanoparticles show the porphyrin coated on AuNPs.

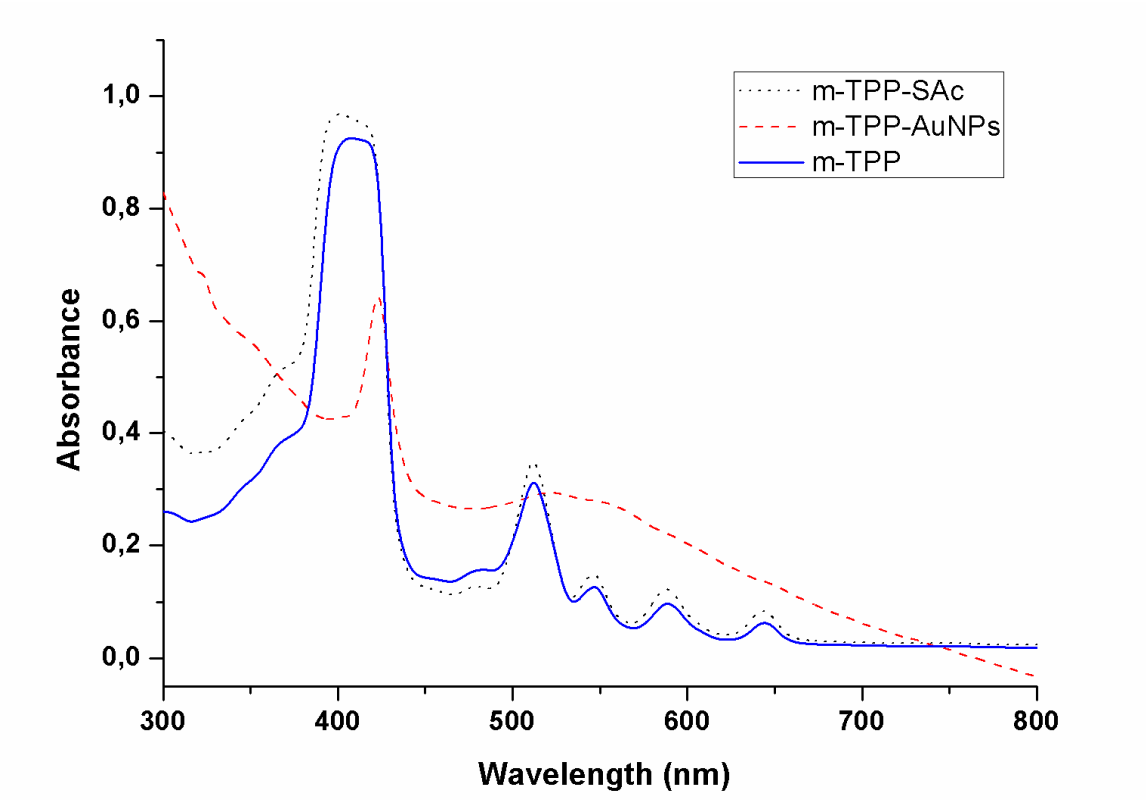

Figure 5.10 m-TPP (solid line), m-TPP-SAc (dotted line) and m-TPP-AuNPs (dashed line)

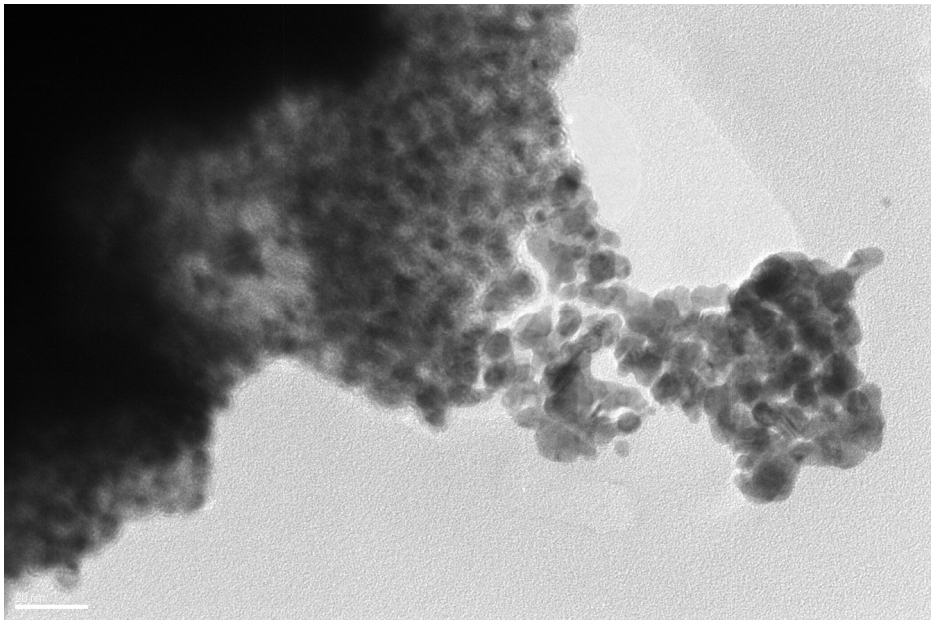

Figure 5.11 TEM image of m-TPP-AuNPs

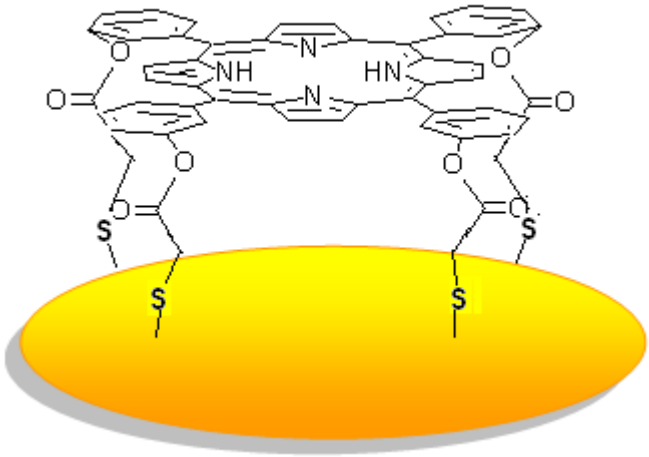

Figure 5.12 m-TPP-AuNPs

5.5 Spectral Characterization of TBP-SAc

Thiol-tailored 4-tert-butyl phenol (TBP-SAc) had been successfully synthesized by the one-pot reaction between TBP, bromoacetyl bromide and potassium thio acetate in THF.

In the IR spectrum of TBP-SAc, characteristic C-O-C and C=O stretching ester groups, came out at 1170 cm^{-1} and 1738 cm^{-1}, respectively. Also, S-C and S-C=O stretching

thio ester groups came out at 1104 cm^{-1} and 1696 cm^{-1}, respectively, as given in the literature for similar compounds. Disappearing of the –OH stretching groups at around 3600-3250 cm^{-1} and the multiple peaks around 3000-2800 cm^{-1} indicated $–CH_2$ and $–CH_3$ aliphatic stretching groups of TBP-SAc.

In the ^{1}H-NMR spectrum of TBP-SAc, the chemical shifts at 2.36 ppm, 3.85 ppm and 1.24 ppm can be attributed to $OC-CH_3$, $OC-CH_2$-S- and CH_3-C- groups (b, c and a), respectively. In addition, the protons on the phenyl group (d and e) were observed at 7.32 (doublet) ppm and 6.97(doublet) ppm, respectively.

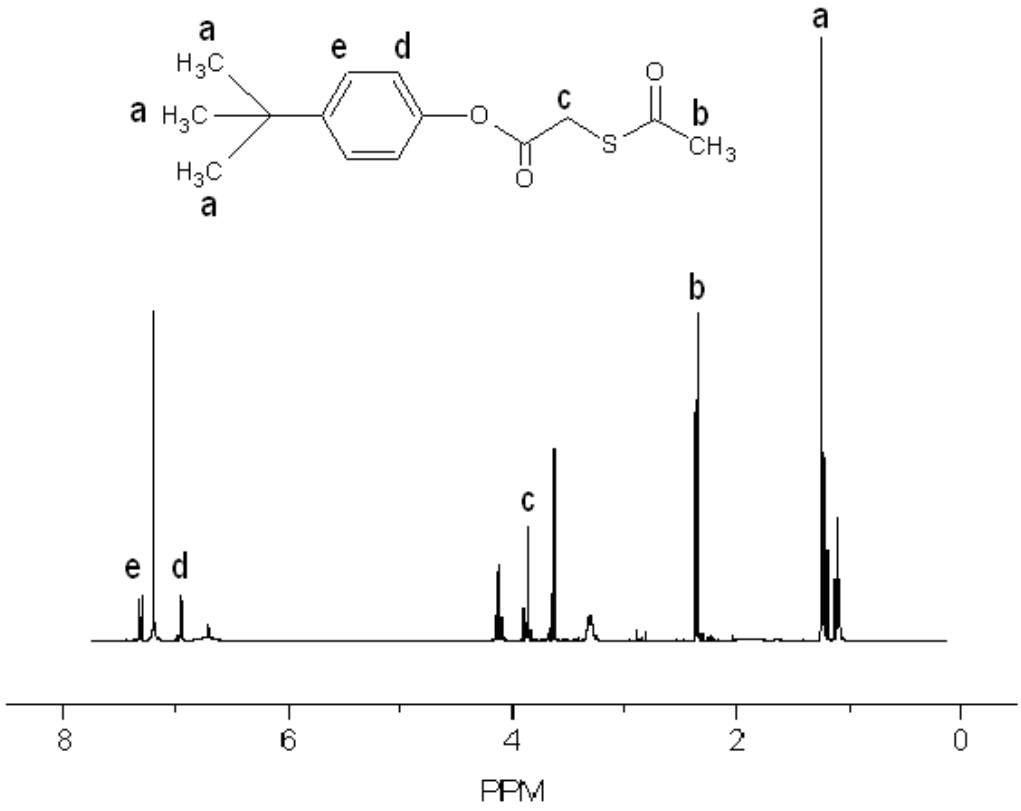

Figure 5.13 ^{1}H-NMR-Spectrum of TBP-SAc

5.6 Spectral Characterization of TBP-AuNPs

TBP-SAc was then coated on AuNPs in the presence of $HAuCl_4$ and $NaBH_4$ in DMF solution.

The newly-synthesized compound (TBP-AuNPs) was characterized by UV-vis. spectrum in which the broad peak (plasmon absorption) around 520 nm indicates the formation of AuNPs (Fig. 5.14).

In the TEM image, the dark-coloured nanoparticles show the porphyrin coated on AuNPs.

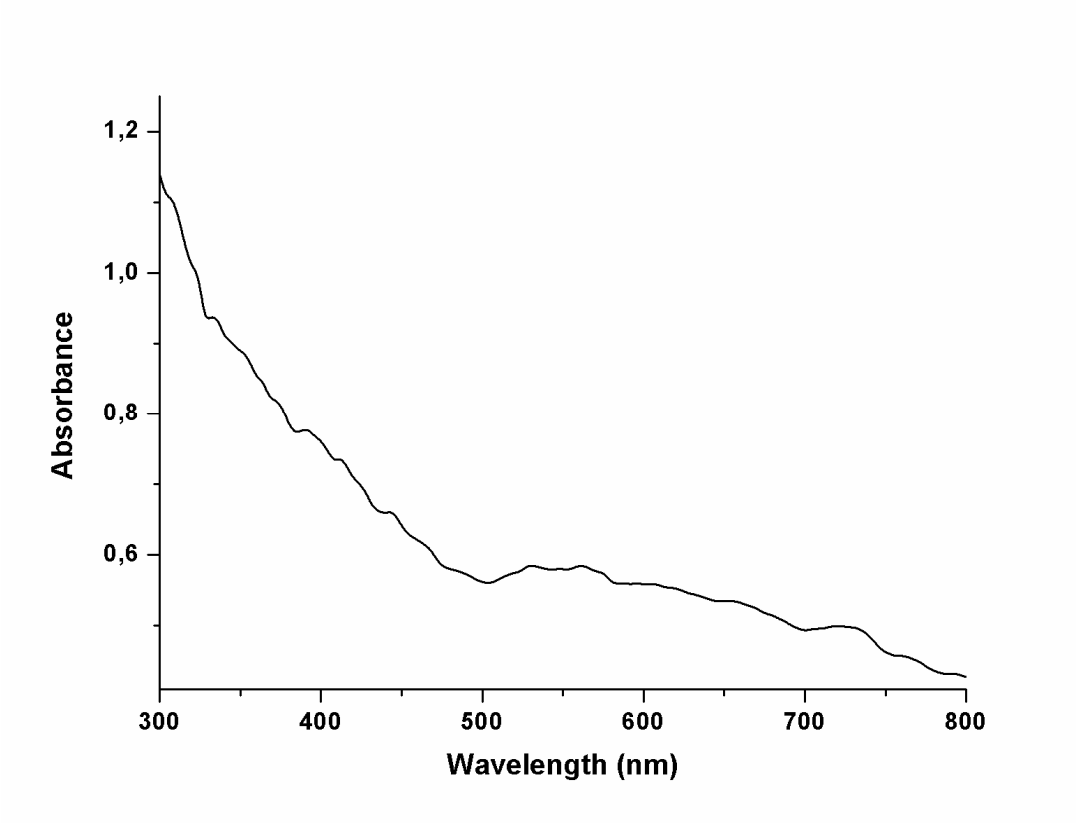

Figure 5.14 UV-vis. spectrum of TBP-AuNPs

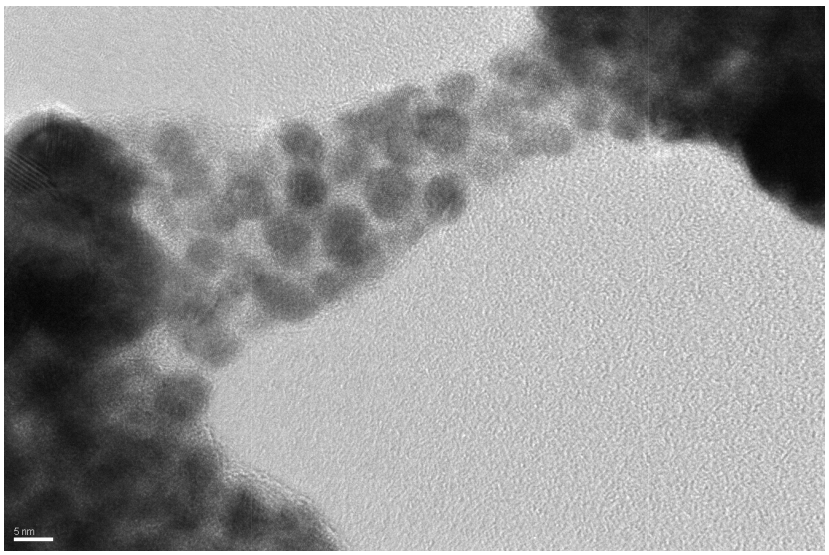

Figure 5.15 TEM image of TBP-AuNPs

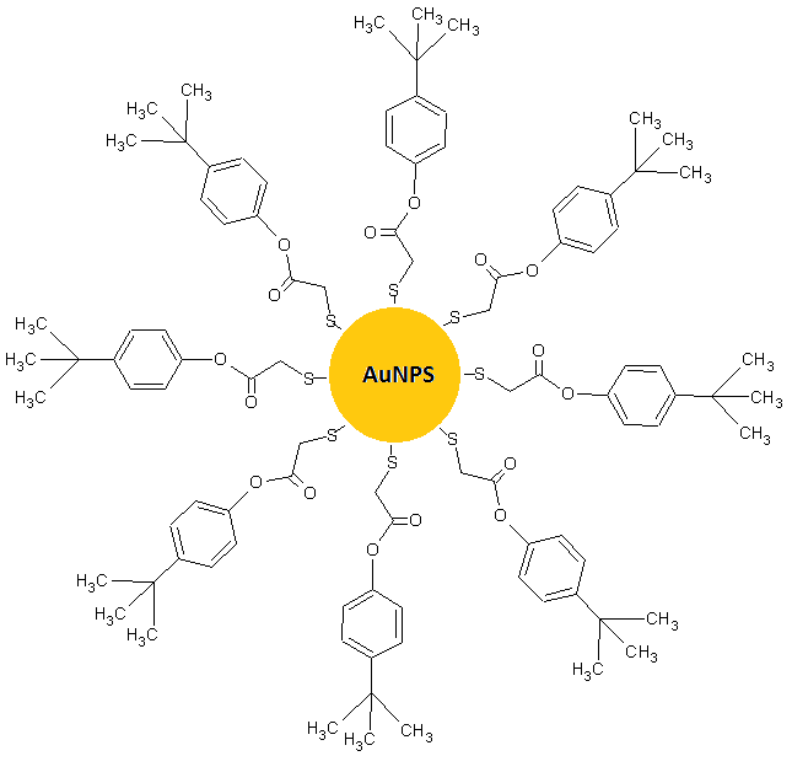

Figure 5.16 TBP-AuNPs

CHAPTER 6

CONCLUSION

Becoming more popular of porphyrin studies, especially in PDT and recent studies of porphyrins coated on AuNPs urged us to investigate the interaction between AuNP and p-conjugated porphyrin systems.

First of all, p-TPP-SAc has been synthesized, and then coated on AuNPs by one-pot reduction of $HAuCl_4$ in the presence of $NaBH_4$ as a reducing agent. p-TPP-AuNPs has been synthesized in a reasonable yield and characterized by UV-vis, TEM, XRD and XPS. Also, its nanoparticle size is found about 10 ±2 nm.

Secondly, m-TPP-SAc has been synthesized, and then coated on AuNPs by one-pot reduction of $HAuCl_4$ in the presence of $NaBH_4$ as a reducing agent.

Thirdly, to control the size of the tetradentate ligands-AuNPs which have smaller in size as compare to monodentate ligands-AuNPs, 4-tert-butyl phenol (TBP) is used as a monodentate passivant. Thiol-tailored monodentate passivant has coated on AuNPs by one-pot reduction of $HAuCl_4$ in the presence of $NaBH_4$ as a reducing agent and characterized by UV-vis. and TEM. The nanoparticle size of TBP-AuNPs is expected to have bigger due to not having steric hindrance. Because of the same reason, disulfide could form instead of TBP-AuNPs.

In conclusion, three different new compounds had been successfully synthesized. The porphyrin derivatives were coated on AuNPs by alternate gold–sulfur self-assembling, which could be used as potential agents in PDT. The tetradentate-AuNPs ones were found smaller in size than the monodentate ligand, since multidentate ligands provide steric hindrance so that small-sized gold nanoparticles are attained, as compared to monodentate ligands.

In further studies, p-TPP-AuNPs and m-TPP-AuNPs could be ideal photosensitizers for PDT.

REFERENCES

[1] R. Rotomskis, R. Augulis, and V. Snitka, *Journal of Physical Chemistry B* 108 (2004) 2833.

[2] L. R. Milgrom, *The Colours of Life: An Introduction to the Chemistry of Porphyrins and Related Compounds*, edited, Oxford University Press, New York, 1997.

[3] T. Arai, K. Takei, N. Nishino, T. Fujimoto, *Chem. Commun.* 1996, 2133.

[4] T. Arai, K. Kobata, H. Mihara, T. Fujimoto, N. Nishino, *Bull. Chem. Soc. Jpn*. 68 (1995) 1989.

[5] H. A. Dailey, *Biosynthesis of Heme and Chlorophylls* McGraw-Hill, New York, 1990.

[6] F. Rabanal, B. R. Gibney, W. F. DeGrado, C. C. Moser, P. L. Dutton, *Inorg. Chim. Acta.* 243 (1996) 213.

[7] G. R. Geier, T. Sasaki, *Tetrahedron Lett.* 38 (1997) 3821.

[8] L. B. Josefsen, R. W. Boyle, *Metal-Based Drugs* 2008 (2007) 1.

[9] J. N. Umbreit, M. E. Conrad, *Am J Hematol.* Aug 64 (2000) 287.

[10] R. F. Pasternack, C. Bustamante, P. J. Collings, A. Giannetto, E. G. Jibbs, *J. Am. Chem. Soc.* 115 (1993) 5393.

[11] I. J. Macdonald, J. Dougherty, *Journal of Porphyrins and Phthalocyanines* 5 (2001) 105.

[12] E. Reddi, M. Ceccon, G. Valduga, G. Jori, J. C. Bommer, F. Elisei, L. Latterini, U. Mazzucato, *Photochemistry and Photobiology* 75 (2002) 462.

[13] R. Murakami, A. Minami and T. Mizutani, *Org. Biomol. Chem.* 7 (2009) 1437.

[14] M. P. Figueroa, J. Santiago, *Photochem. Photobiol. Sci.* 3 (2004) 33.

[15] P. Rothemund, *J. Am. Chem. Soc*. 58 (1936) 625.

[16] P. Rothemund, *J. Am. Chem. Soc.* 57 (1935) 2010.

[17] A. D. Adler, F. R. Longo, J. D. Finarelli, J. Goldmacher, J. Assour, L. Korsakoff, *J. Org. Chem.* 32 (1967) 476.

[18] R. E. Falvo, L. M. Mink, D. F. Marsh, *J. Chem. Educ.* 76 (1999) 237.

[19] L. D. Dobbins, N. Ravi, Ph.D., Albert N. Thompson, Jr, Ph.D, *Mossbauer spectroscopic charecterization of a water soluble porphyrin*, Department of chemistry, United States, 1998.

[20] A. F. Mironov, M. A. Grin, A. G. Tsiprovskiy, V. V. Kachala, T. A. Karmakova, A. D. Plyutinskaya, Raisa I. Yakubovskaya, *Journal of Porphyrins and Phthalocyanines* 7 (2003) 725.

[21] L. Feng, L. Tianjun, W. Li, *Springer Berlin Heidelberg* 19 (2008) 186.

[22] Q. Peng, J. Moan, L. W. Ma, J. M. Nesland, *Cancer Research* 55 (1995) 2620.

[23] Y. Shiraishi, *Synthesis of novel metal nanoparticles and their application to nano-optical materials*, Research Scientist, Tokyo University of Science, 2004.

[24] G. A. Ozin, A. C. Arsenault, *Nanochemistry*, edited, RSC Publishing, Cambridge, 2005.

[25] M. Stemmler, F. D. Stefani, S. Bernhardt, R. E. Bauer, M. Kreiter, K. Müllen, W. Knoll, *Langmuir* 25 (2009) 12425.

[26] J. Deka, A. Paul, A. Ramesh, A. Chattopadhyay, *Langmuir* 24 (2008) 9945.

[27] S. Link, M. A. El-Sayed, *Int. Rev. Phys. Chem.* 19 (2000) 409.

[38] A. Ishida, T. Majima, *Chem. Phys. Lett.* 322 (2000) 242.

[39] N. Fukuda, M. Mitsuishi, A. Aoki, T. Miyashita, *J. Phys. Chem. B* 106 (2002) 7048.

[30] M. Nuruzzaman, T. C. Preston, S. Mittler, N. D. Jones, *Synlett* 2008, 207-212.

[31] S. Link, M. A. El-Sayed, *Int. Re*V. *Phys. Chem.* 19 (2000) 409.

[32] Y. N. Hwang, D. H. Jeong, H. J. Shin, D. Kim, S. C. Jeoung, S. H. Han, J. S. Lee, G. J. Cho, *Phys. Chem. B* 106 (2002) 7581.

[33] E. Dulkeith, T. Niedereichholz, T. A. Klar, J. Feldmann, G. von Plessen, D. I.Gittins, K. S. Mayya, F. Caruso, *Phys. Re*V. *B* 70 (2004) 205424.

[34] R. A. Sperling, P. R. Gil, F. Zhang, M. Zanella, W. J. Parak, *Chem. Soc. Rev.* 37 (2008) 1896.

[35] S. S. Zhang, G. Leem, L. O. Srisombat, T. R. Lee, *J. Am. Chem. Soc.* 130 (2008) 113.

[36] A. A. Yasseri, D. Syomin, V. L. Malinovskii, R. S. Loewe, J. S. Lindsey, F. Zaera, D. F. Bocian, *J. Am. Chem. Soc.* 126 (2004) 11944.

[37] M. Kanehara, H. Takahashi, T. Teranishi, *Angew. Chem.* 120 (2008) 313.

[38] J. Ohyama, Y. Hitomi, Y. Higuchi, M. Shinagawa, H. Mukai, M. Kodera, K. Teramura, T. Shishidoa, T. Tanakaa, *Chem. Commun.* 2008, 6300–6302.

[39] M. Kanehara, T. Teranishi, *e-J. Surf. Sci. Nanotech. 3 (2005) 30.*

[40] K. Szaciłowski, W. Macyk, A. Drzewiecka-Matuszek, M. Brindell, G. Stochel, *Chem. Rev.* 105 (2005) 2647.

[41] D. O. Cowan, R. L. Drisko, *Elements of Organic Photochemistry*, edited, Plenium Press, NewYork and London, 1976.

[42] R. M. Ion, *Rom. J. Biophys.* 6 (1996) 205.

[43] M. Lovcinsky, J. Borecky, P. Kubat, P. Jezek, *Gen. Physiol. Biophys.* 18 (1999) 107.

[44] M. C. Berenbaum, S. L. Akande, R. Bonnett, H. Kaur, S. Ioannou, R. D. White, U. J. Winfield, *Br. J. Cancer* 54 (1986) 717.

[45] T. Wejrzanowski, R. Pielaszek, A. Opalinska, H. Matysiak, W. Łojkowski, K.J.Kurzydłowski, *Appl. Surf. Sci.* 253 (2006) 204.

[46] R. Pielaszek, "Analytical expression for diffraction line profile for polydispersive powders," in *Proceedings of the 19th Conference on Applied Crystallography*, Kraków, Poland, September 2003.

[47] M. R. Shadnam and A. Amirfazli, *Chem. Commun.* 2005, 4869–4871.

[48] L. JunHua, Y. JingZhong, X. XueSong, A. Indira, "Studying Package Delamination by TOF-SIMS and XPS" in *CS MANTECH Conference*, Austin, Texas, USA, May 14-17, 2007.

[49] H. Hamoudi, M. Prato, C. Dablemont, O. Cavalleri, M. Canepa, V. A. Esaulov, *Langmuir* 26 (2010) 7242.

APPENDIX A

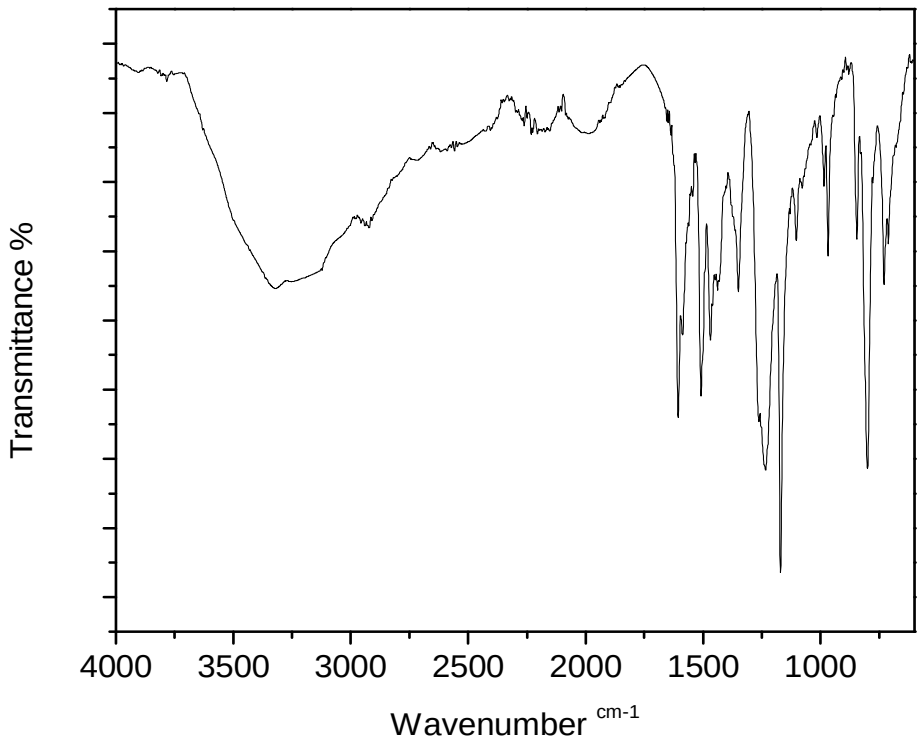

IR Spectrum of p-TPP

APPENDIX B

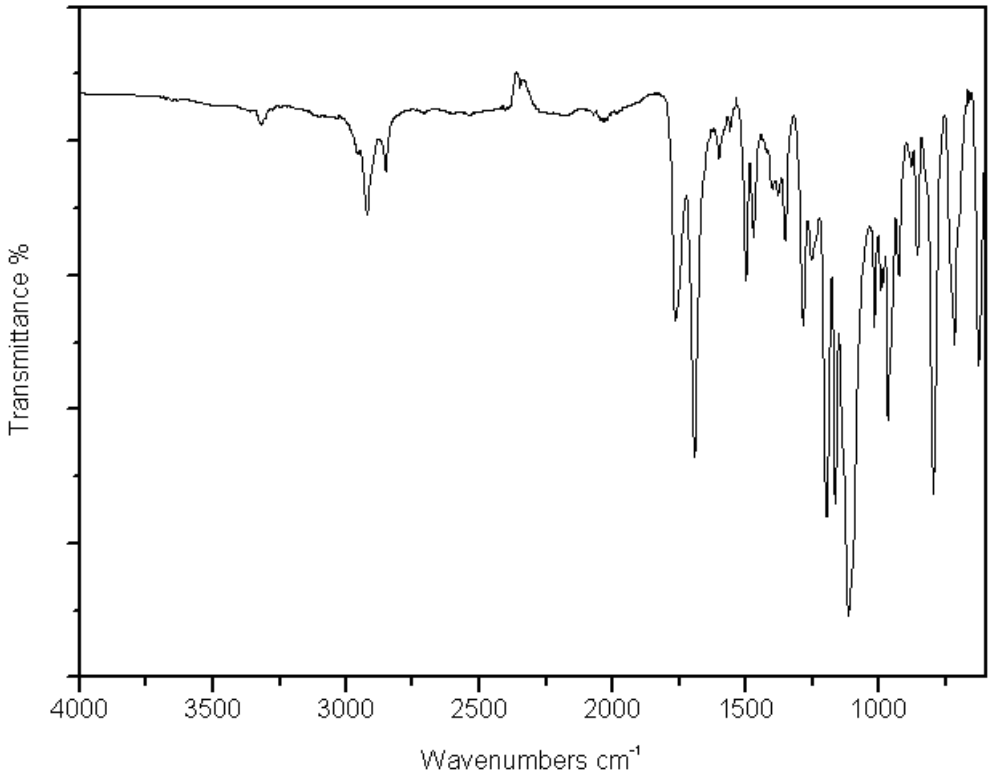

IR Spectrum of p-TPP-SAc

APPENDIX C

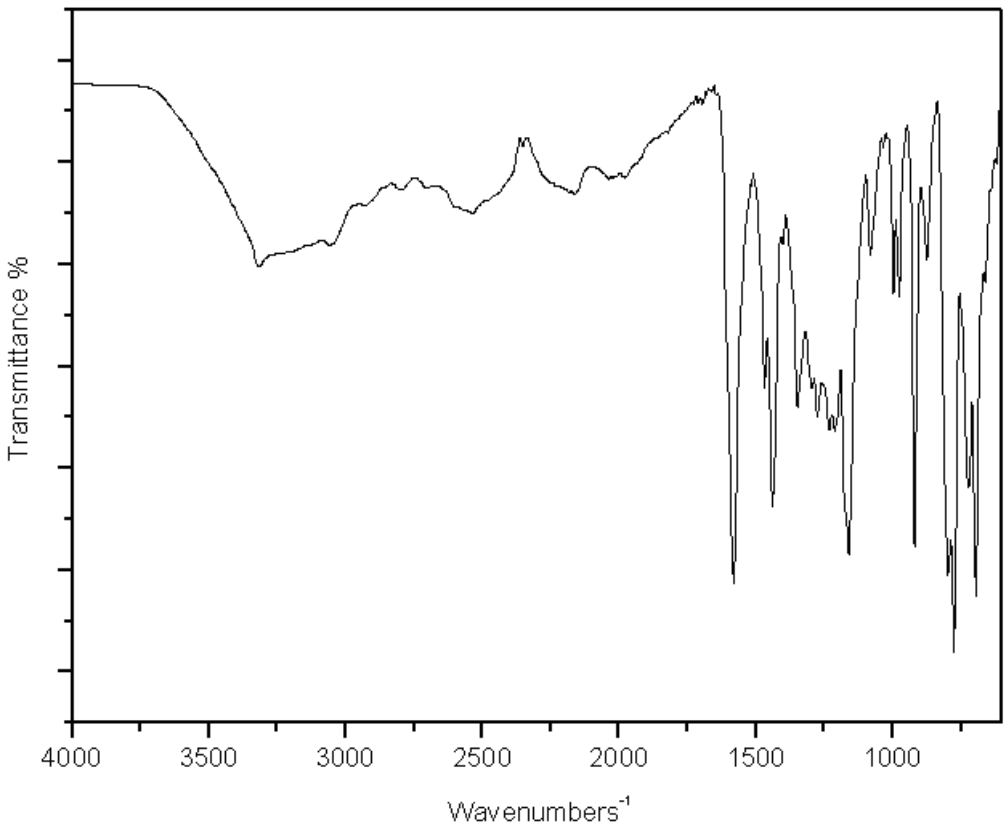

IR Spectrum of m-TPP

APPENDIX D

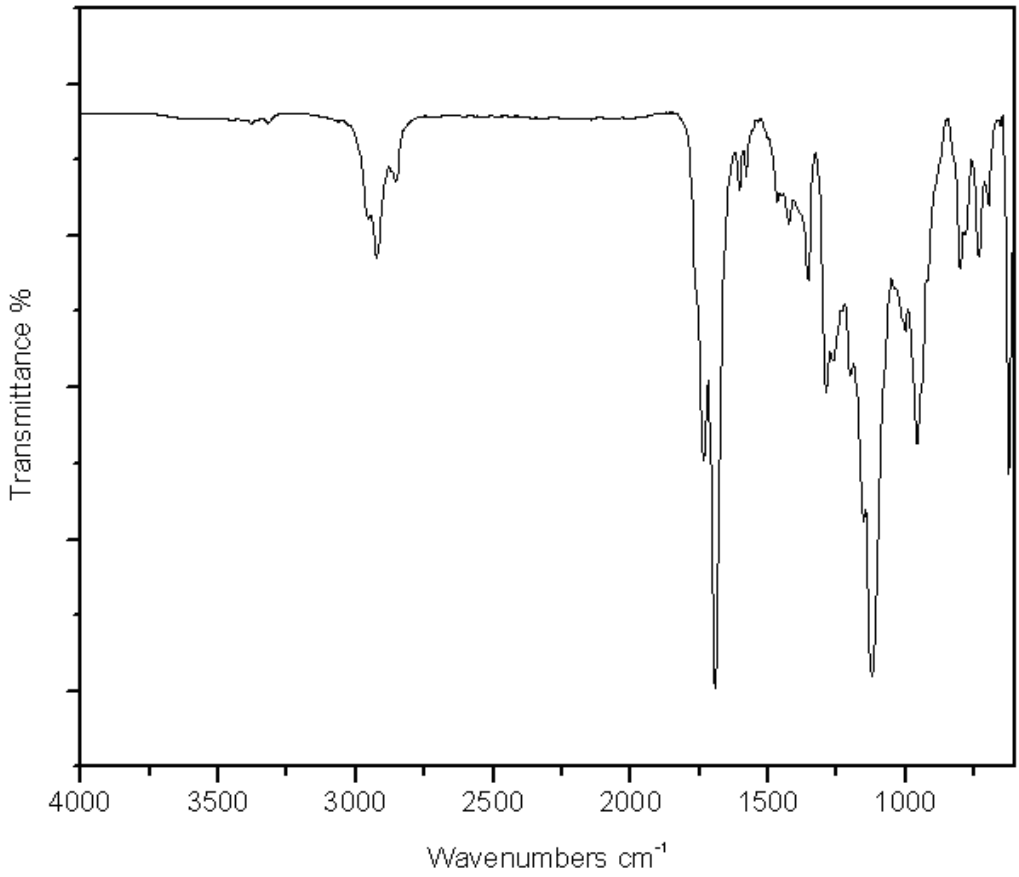

IR Spectrum of m-TPP-SAc

APPENDIX E

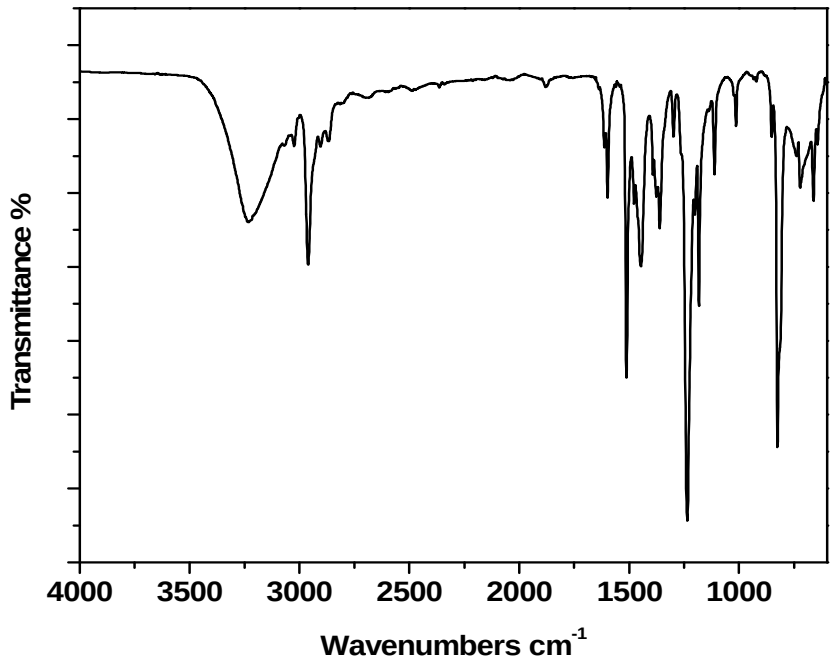

IR Spectrum of TBP

APPENDIX F

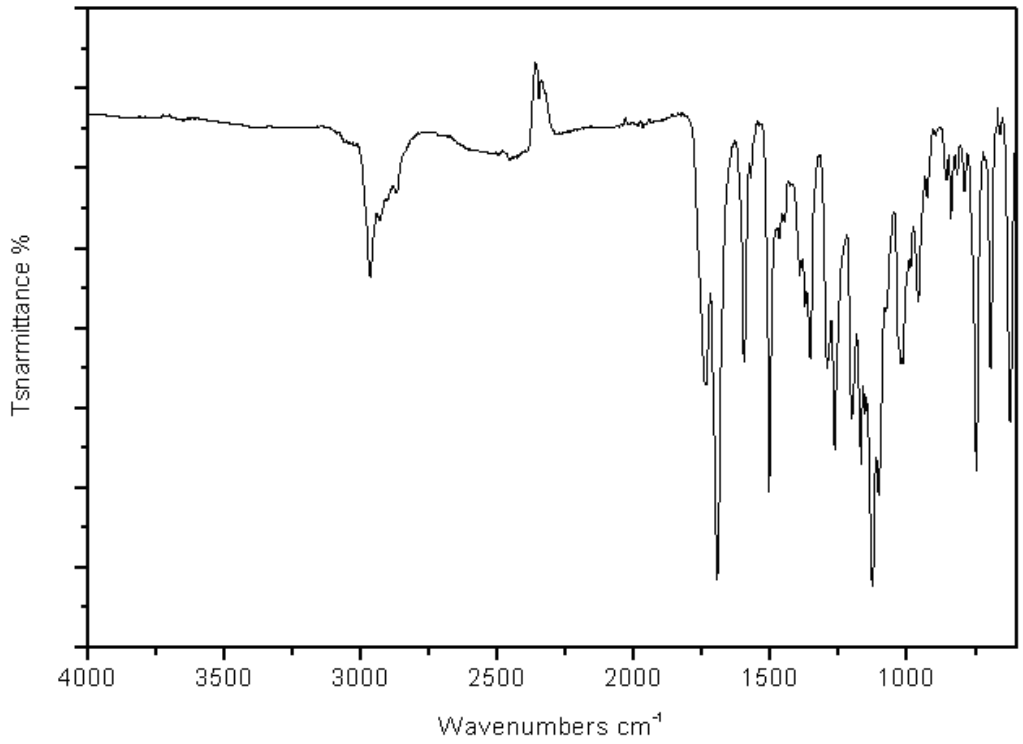

IR Spectrum of TBP-SAc

APPENDIX G

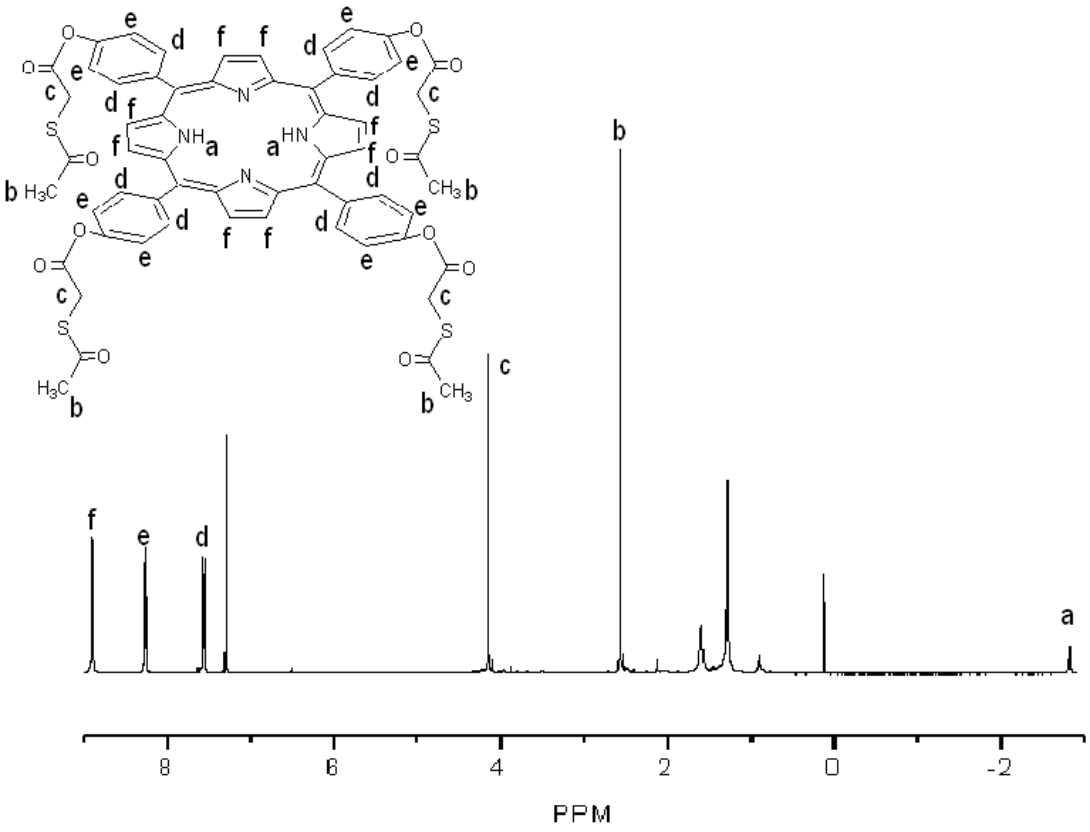

^{1}H-NMR-Spectrum of p-TPP-SAc

APPENDIX H

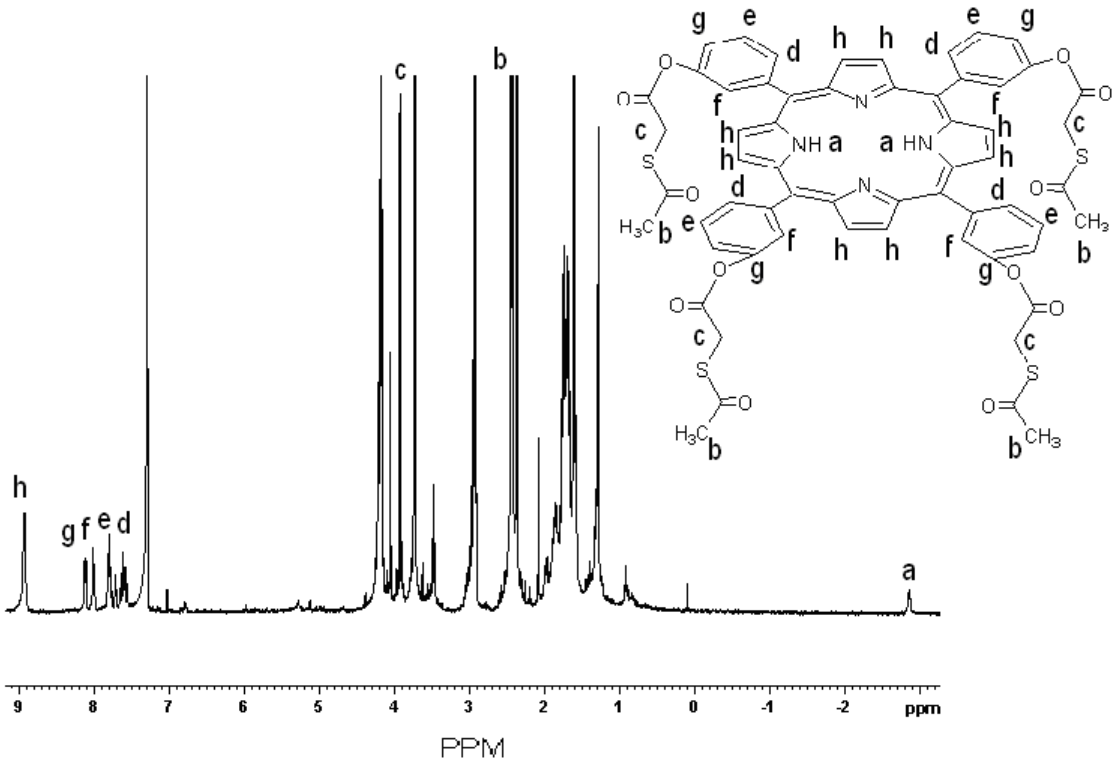

^{1}H-NMR-Spectrum of m-TPP-SAc

APPENDIX I

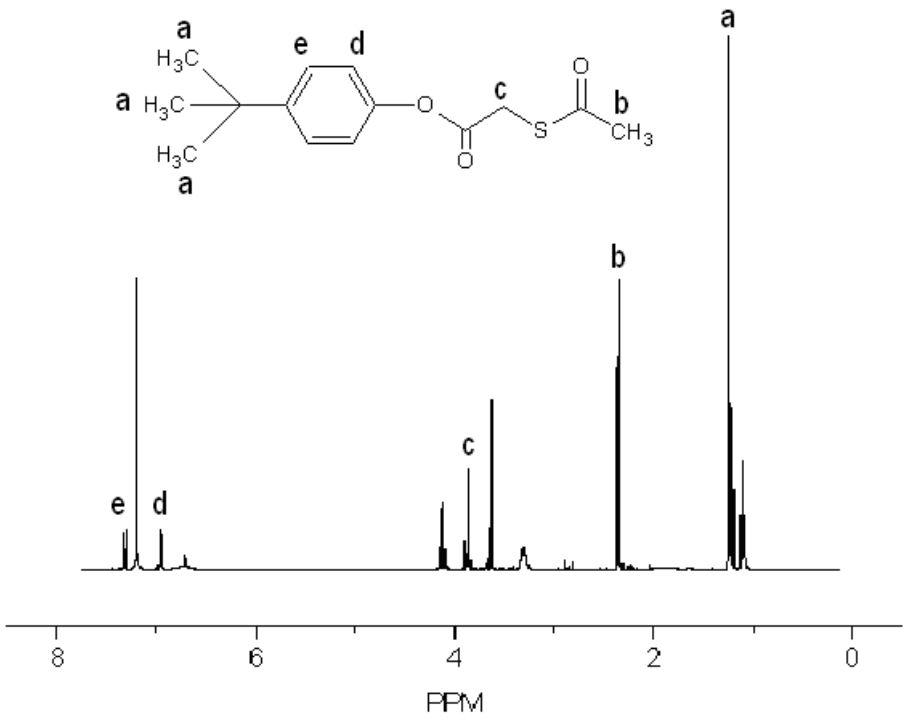

^{1}H-NMR-Spectrum of TBP-SAc

APPENDIX J

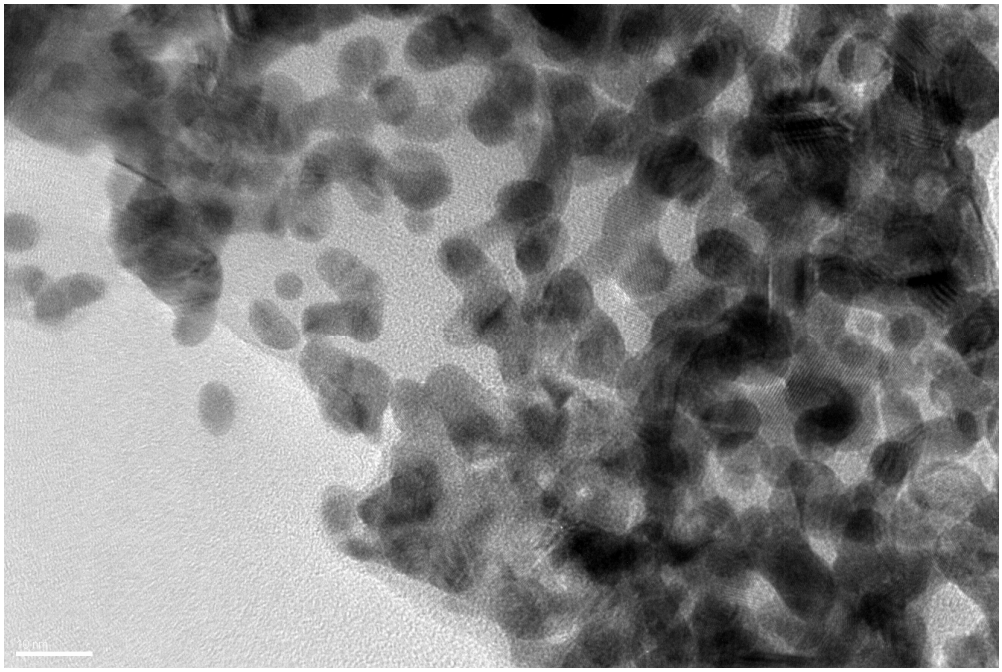

TEM image of p-TPP-AuNPs

APPENDIX K

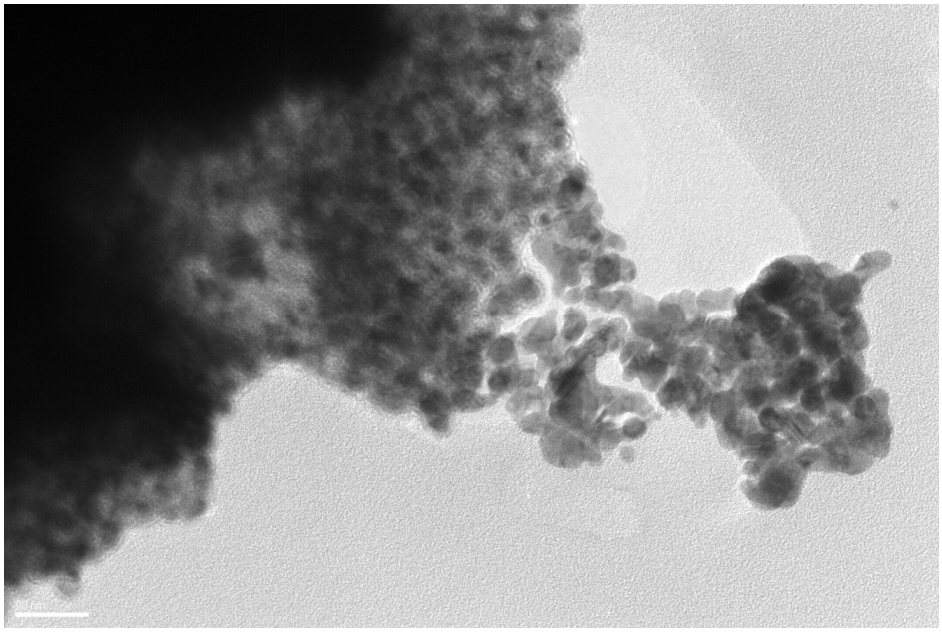

TEM image of m-TPP-AuNPs

APPENDIX L

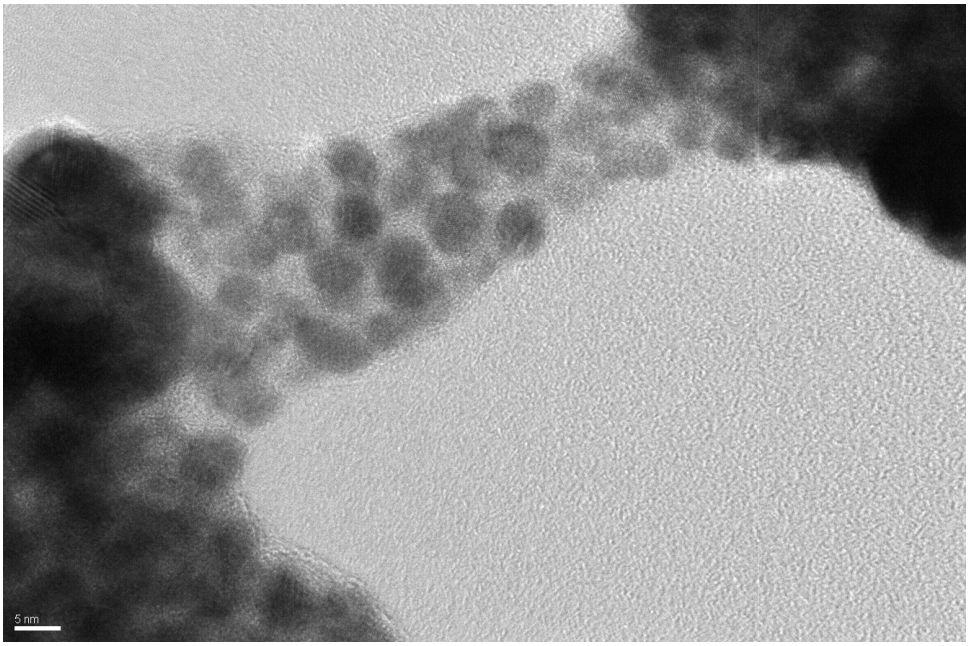

TEM image of TBP-AuNPs

APPENDIX M

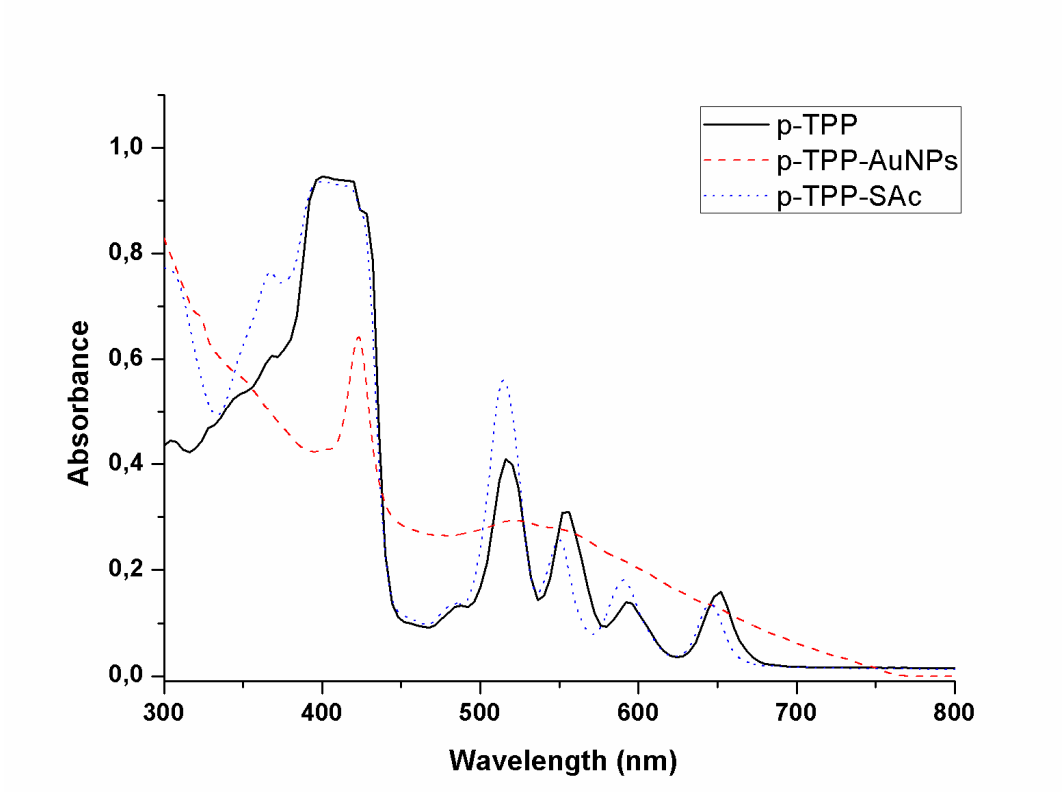

UV-vis. Spectra of p-TPP (solid line), p-TPP-SAc (dotted line) and p-TPP-AuNPs (dashed line)

APPENDIX N

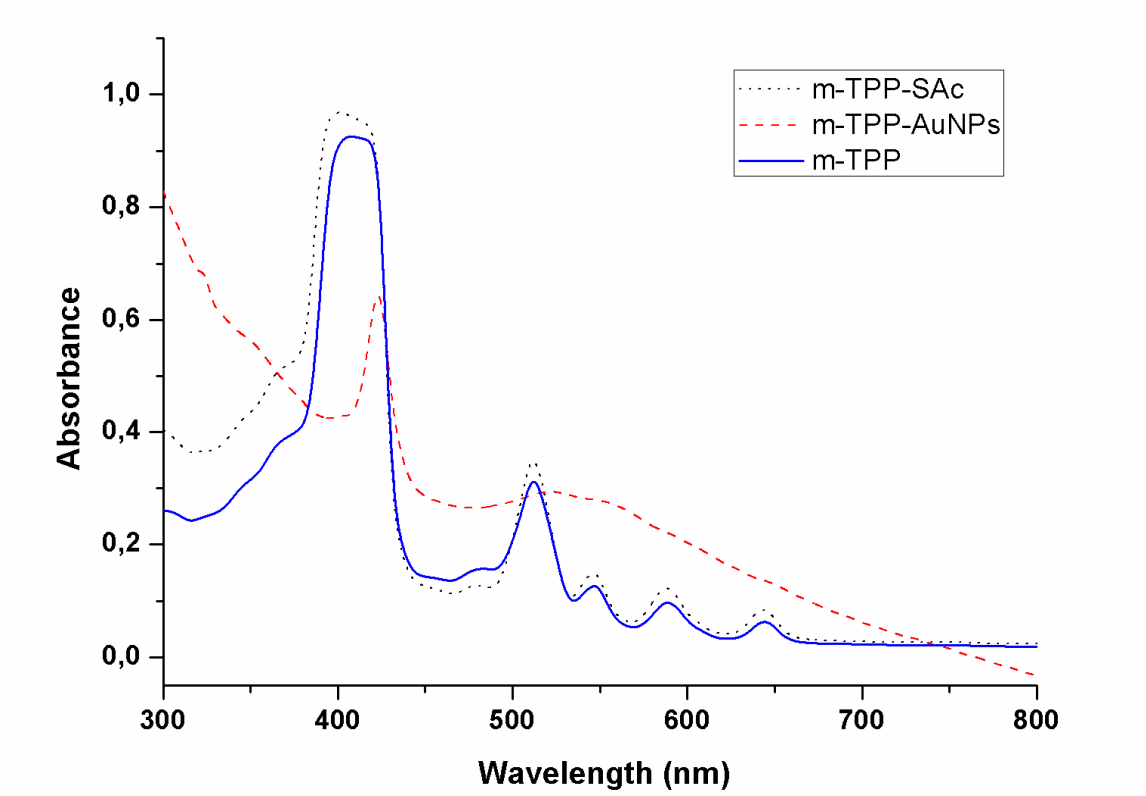

UV-vis. Spectra of m-TPP (solid line), m-TPP-SAc (dotted line) and m-TPP-AuNPs (dashed line)

APPENDIX O

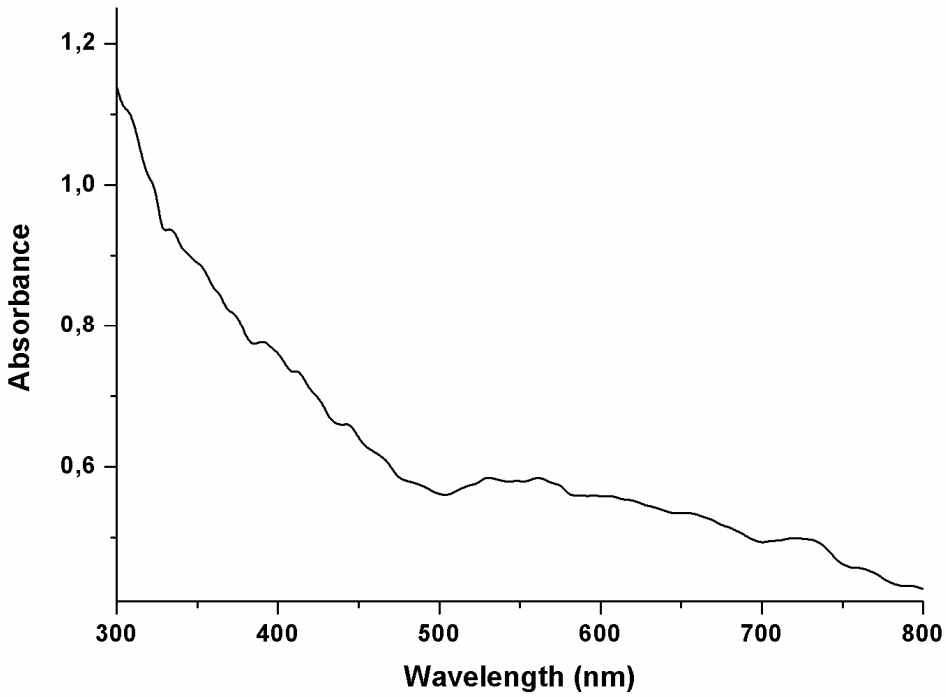

UV-vis. Spectrum of TBP-AuNPs

APPENDIX P

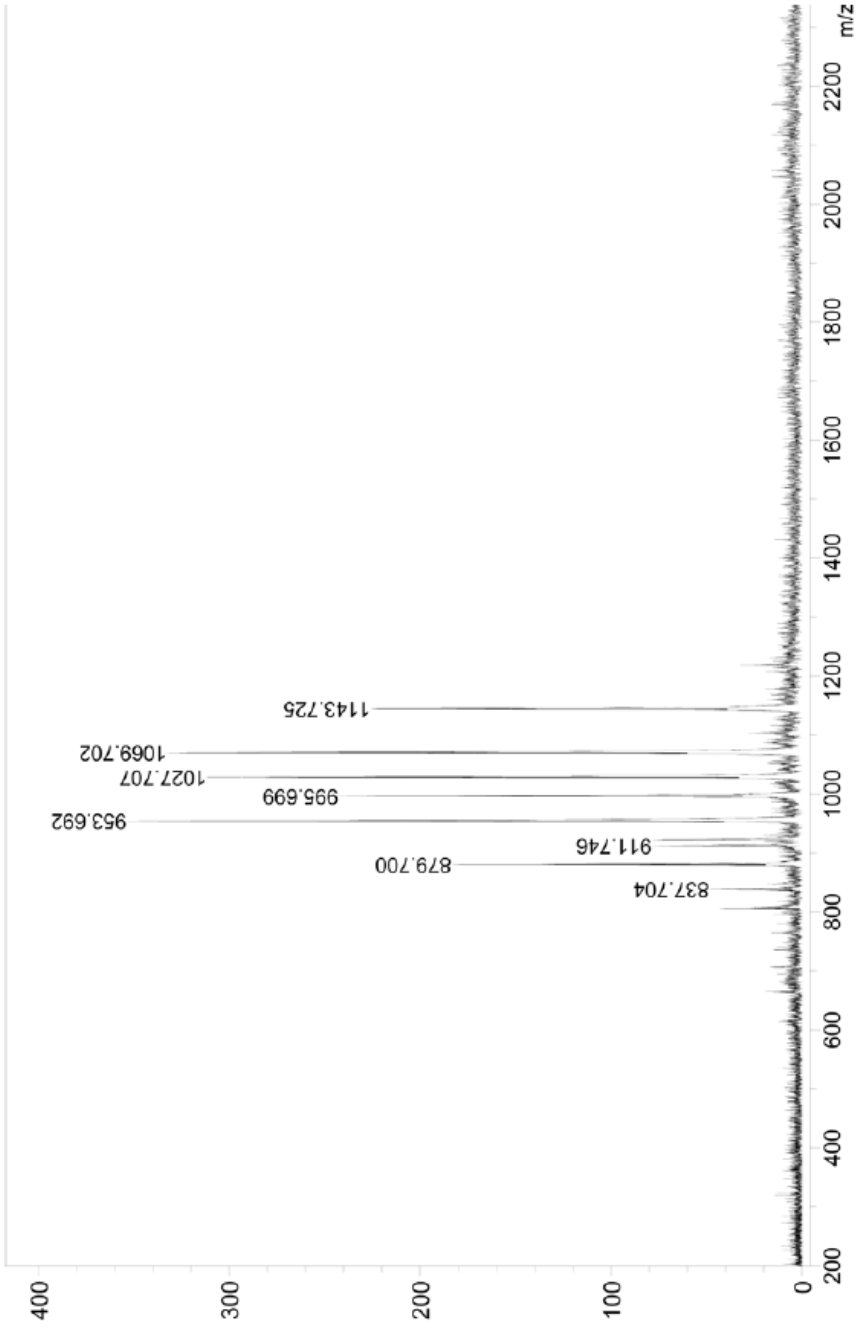

Mass Spectrum of p-TPP-SAc

APPENDIX R

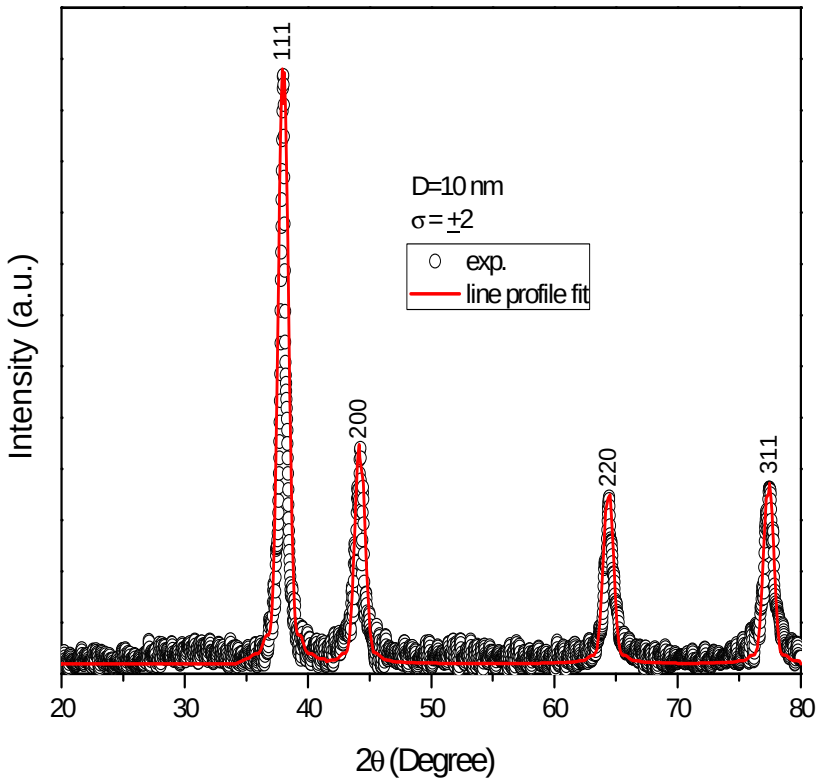

XRD Spectrum of p-TPP-AuNPs

APPENDIX S

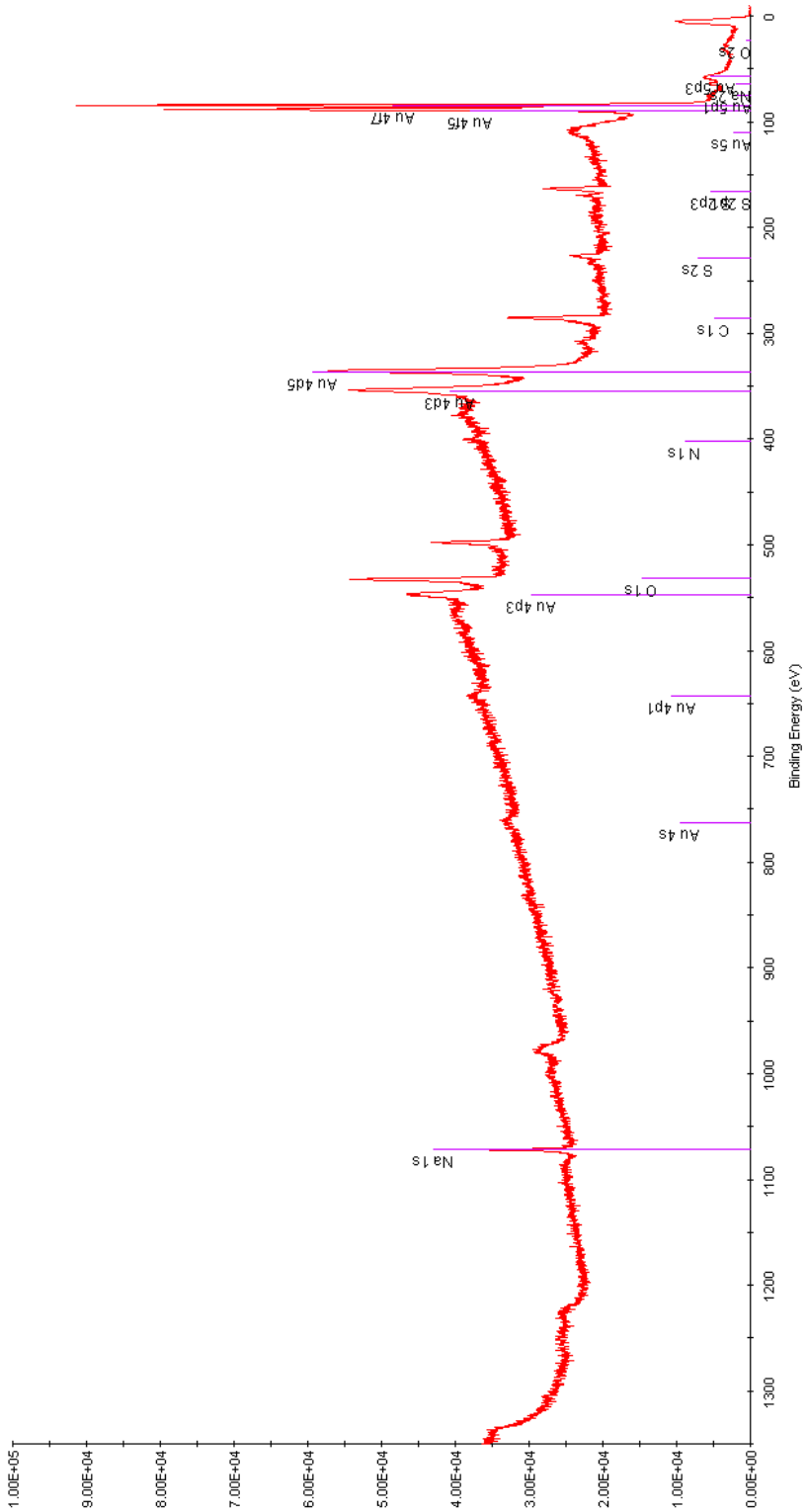

XPS Spectrum of p-TPP-AuNPs